A plant-derived nucleic acid protects mice from respiratory viruses in an IFN-I-dependent and independent manner

Dacquin, Muhandwa KASUMBA

Table of content

Pages

Abstract

Pathogen-associated molecular patterns (PAMPs) are activators of immunity in mammalian cells. Among the various PAMPs signatures currently known double-stranded RNA (dsRNA) structures are the chief signal for host immune sensors upon RNA virus invasion. Synthetic dsRNA have been used to activate antiviral immunity. Such strategy is limited by the difficulty to enzymatically synthetize high molecular weight (HMW) dsRNA. Although molecules such as poly I:C have been useful, their unnatural and uncharacterized structure remain a concern. To address this issue, a naturally-occurring HMW dsRNA extracted from rice-bran (rb-dsRNA) was tested for immune stimulation. This nucleic acid induced expression of interferons (IFNs) and stimulated genes involved in innate immunity both *in vitro* and in murine lungs. Alveolar macrophages were the main producers of type-I IFN in the lungs in response to rb-dsRNA. The nucleic acid induced a strong protection against respiratory viruses (IAV and Sendai virus) by signaling through TRIF and IPS-1 via TLR3 and MDA5 respectively. Interestingly, IFNAR1-deficient mice retained a residual protection which was abolished by caspase-1 inhibition but not by inhibition of IL-1 signaling. In fact, rb-dsRNA also activated caspase-1 via TRIF, thereby driving a pyroptotic-like cell death of alveolar macrophages. Cleavage of gasdermin D, as an indicator of pyroptosis, was also confirmed. The reported data suggest that rb-dsRNA is potent activator of innate immunity and is capable of protecting mice against lethal infection of respiratory viruses in an IFN-dependent and independent manner.

Abbreviations

AMΦ: *alveolar macrophage*

BALF: *bronchoalveolar lavage fluid*

BM-MΦ: *bone marrow–derived MΦ*

DKO: *double KO*

IAV: *influenza A virus*

IFN-I: *type I IFN*

IL1RA: *IL-1R antagonist*

IMΦ: *interstitial MΦ*

i.n.: *intranasal(ly)*

i.p.: *intraperitonial(ly)*

ISG: *IFN-stimulated gene*

KO: *knockout*

LDH: *lactate dehydrogenase*

MΦ: *macrophage*

MDA5: *Melanoma differentiation-associated protein 5*

MEF: *mouse embryonic fibroblast*

PAMP: *pathogen-associated molecular pattern*

p.i.: *postinfection*

poly I:C: *polyinosinic-polycytidylic acid*

rb-dsRNA: *dsRNA extracted from rice bran*

RIG-I: *Retinoic acid-inducible gene I*

RLR: *Rig-I-like receptor*

RT-qPCR: *real-time quantitative PCR*

TLR3: *Tool-like receptor 3*

SeV: *Sendai virus*

WT: *wild-type.*

Chapter 1

INTRODUCTION

1.1. Innate immunity and viral nucleic acids

Innate immunity in mammalian cells is a complex cascade of events initiated upon sensing of pathogen-associated molecular patterns (PAMPs) which are considered as danger signals by the host cell. While some viruses display PAMPs on their genetic materials, which are recognized as foreign by host immune receptors, others generate such structures or patterns during replication. Recognition of PAMPs, such as double-stranded RNA structures, triphosphate containing nucleic acids, unconventional nucleic acid structures or bacterial structures, by toll-like receptors (TLRs) or RIG-I-like receptors (RLRs) activates signal transduction pathways which culminate in the production of antiviral effector molecules capable of stemming the spread of pathogens[1, 2, 3].

It is widely accepted that viral nucleic acids constitute the primary activator of immune response upon virus infection. Viral nucleic acids and their derivatives are recognized by cytosolic receptors such RLRs (i.e. RIG-I and MDA5) and DNA sensors (i.e. cGAS and DAI) or DNA sensors in the nucleus. The RNA helicases retinoic acid-inducible gene I (RIG-I) and melanoma-differentiation-associated protein 5 (MDA5) signal through their common adaptor mitochondrial antiviral-signaling protein (MAVS) commonly called interferon promoter stimulator-1 (IPS-1). While on the other hand, DNA sensors such as Cyclic GMP-AMP synthase (c-GAS) and DNA-dependent activator of IFN-regulatory factors (DAI) require the adaptor molecule stimulator of interferon gene (STING). Such signal transduction culminates in the phosphorylation and nuclear translocation of transcription factors

(e.g. IRF3 and IRF7) resulting in the transcriptional induction of interferon genes[4, 5]. Type I interferon (IFN-I) is considered the main antiviral cytokine capable of inducing a large number of other protective molecules commonly referred to as interferon-stimulated genes (ISGs)[6, 7, 8]. The activation of antiviral immune responses is also associated with a range of inflammatory signals that trigger the induction of inflammatory cytokine genes through NF-kappaB transcription factor, activation of caspases, production of reactive oxygen species and recruitment of inflammatory cells[9, 10, 11, 12].

1.2. Viral RNA analogues and innate immunity activation

Although host nucleases (i.e. RNases and DNases) act as guard rails preventing unnecessary and excessive activation of immune response upon virus infection, dsRNA has demonstrated stronger immune stimulating capacity than dsDNA. This is probably because of the strong stability of the former, directly correlated to the presence of 2'OH making dsRNA molecules more rigid. For such reasons viral RNA analogues have been immune stimulants of choice in immunological studies allowing researchers to investigate components of the antiviral immune system.

For decades, simulation of virus infection and replication has been achieved by the use of synthetic dsRNA, represented by poly I:C. Since the late 60's, the use of such analogues has helped to elucidate key components of antiviral immunity[13, 14, 15, 16, 17]. Historically, immune protection induced by such artificial

analogues has been attributed almost exclusively to IFNs, without considering inflammatory events therefore raising questions about their accuracy to mimic viral RNA. Furthermore, poly I:C has been shown to be unstable in body fluid; this has been a challenge limiting its *in vivo* and clinical application. Although attempts to stabilize poly I:C are been sought[15, 18], the artificial nature of the molecule remains a concern to many. In fact, poly I:C is composed of non-physiological poly I and poly C found nowhere in nature.

1.3. Viral RNA activates inflammasome in the respiratory tract

The cascade of events involved in the immune response differs slightly between tissues and organs. The respiratory tract, for example, is home to numerous immune cells. Upon infection and inflammation, circulating immune cells are quickly recruited to help mount a strong immune reaction[9, 11]. Although the central role of IFN-I has long been recognized in the antiviral response, recent reports have shed light on the contribution of inflammatory events[10, 19, 20, 21, 22, 23, 24, 25, 26]. Particular attention has been given to the recently observed inflammasome activation driven by viral RNA (and analogues) recognition by immune receptors. It is now accepted that recognition of viral RNA species in the respiratory tract activates caspases and cell deaths as part of the host immune response[10, 19, 22, 24]. In fact, reports have demonstrated that inflammasome and caspase-1 activation as a result of viral RNA recognition significantly contributes to mounting an efficient antiviral response. Although a previous report demonstrated the direct role of

NLRP3 inflammasome activation, the detailed mechanism behind such antiviral response is still elusive[19]. Furthermore, direct evidence linking inflammasome and caspase activation by viral RNA analogues, such as poly I:C, to immunity has been lacking thereby raising even more questions about the ability of the artificial molecule to accurately mimic viral dsRNA.

1.4. Endornaviridae in plants: the tale of a neglected alternative

In the hope of addressing the limitations associated with synthetic dsRNA molecules in *in vivo* settings, the use of *Endornaviridae* as a natural approach accurately mimicking viral dsRNA was considered. This naturally-occurring long (about 14 kbp) dsRNA, a genome of *Endornavirus,* is found in several plants[27, 28, 29, 30, 31, 32] and some species of fungi[33]. In plants, endornaviruses are transmitted vertically through pollens and ova without causing any notable disease. Although classified as a virus, this naked dsRNA is not infectious and has been reported to encode a single protein. This plasmid-like dsRNA is found in several edible plants such as some species of rice and bell-shaped green peppers therefore solidifying clams about its safety.

I used dsRNA extracted from rice bran in this study. The findings suggest that dsRNA extracted from rice bran (rb-dsRNA) is a potent activator of innate immunity. Additionally, rb-dsRNA modulated immunity against respiratory viruses, such influenza A (IAV) and murine parainfluenza type I virus (Sendai virus), thereby protecting mice from virus-induced morbidity and mortality. Both IFN-I

signaling and caspase-1 activation contributed to the protection against virus infection. Furthermore, because of its natural nucleotide sequence[34], I propose that rb-dsRNA could be a more accurate mimic of viral RNA for immunological studies. Additionally, this is the first study reconciling IFN-I and an inflammatory event in antiviral immune protection driven by a nucleic acid mimicking replicating viruses.

Chapter 2

MATERIALS AND METHODS

2.1. Animals, cells, viruses, reagents, and antibodies

Mice used throughout the study were female 6 to 8 weeks-old. Influenza A virus (A/PR/8/34 H1N1) was propagated in fertilized chicken eggs and the titer was quantified using standard plaque assay with Mardin-Darby canine kidney MDCK cells. Sendai virus (Cantell strain) was propagated in HEK293T cells and titer quantified using standard plaque assay with Vero cells. The following antibodies were used; purified rat anti-mouse CD16/CD32 clone 2.4G2 (BD Biosciences), anti-mouse F4/80 clone BM8 (BioLegend), anti-mouse SiglecF clone M1304A01 (BioLegend), anti-mouse CD11c clone N418 (BioLegend), anti-mouse CD11b clone M1/70 (BioLegend), anti-mouse Ly-6G clone 1A8 (BioLegend), anti-mouse Ly-6C clone HK-1.4 (Biolegend) anti-influenza A NP clone A1 (Millipore), anti-human Influenza A, B, rabbit polyclonal (Takara Bio Inc.), anti-caspase-1 p10 clone M-20 (Santa Cruz) and anti-GSDMDC1 clone A-7 (Santa Cruz).

2.2. Extraction of dsRNA from Oryza sativa japonica Koshihikari

A volume of 300 ml of buffer containing 0.1 M NaCl and 10 mM CH_3COONa and 0.5% sodium deoxycholate was vigorously mixed with 60 g of Oryza sativa japonica Koshihikari rice bran and centrifuged at 10,000 rpm for 10 minutes. The supernatant was collected and subjected to phenol-chloroform treatment. Total nucleic acid was precipitated from the water phase using isopropanol (1:1). The pellet was washed once with 70% ethanol, vacuum dried, and re-suspended in TE buffer pH 7.5. The precipitated nucleic acid was fractionated using 6 M LiCl to purify the high molecular weight nucleic acid.

2.3. Intranasal administration and infection

Mice were anaesthetized with pentobarbital (i.p.) before intranasal administration of 30 µl inoculum per mouse. Respective inocula contained 20 µg of rb-dsRNA, influenza A (IAV) virus (PR/8), Sendai virus (Cantell strain), any other treatment (clodronate liposome, monoclonal antibodies, etc.), or the same of volume of PBS as control.

Mice were infected with 1000 pfu of IAV except when otherwise indicated. For survival experiments 200 pfu of IAV was used. For the Sendai virus, 3000 pfu of the virus was used throughout the study.

2.4. Plaque assay for *Influenza* A virus H1N1 PR/8

Virus titers in infected lungs were determined using standard plaque assay. Briefly, confluent monolayers of Mardin-Darby canine kidney (MDCK) cells were incubated with serum-free Eagle's MEM containing serial amount of influenza virus respectively for 1 h at 37°C in 5% CO_2. The cells were overlaid with DMEM-diluted 0.6% agar and maintained in at 37°C and 5% CO_2 for 2 to 3 days. For PR/8 the agar overlay was supplemented with 1 µg/ml TPCK-treated trypsin. The monolayer was stained with crystal violet and the number of plaques counted.

2.5. RT-qPCR

Total RNA was extracted from cells or tissues using TRIzol reagent (Invitrogen Life Technologies) and subjected to DNase I treatment before 200 ng of total RNA was reverse-transcribed with MultiScribe reverse transcriptase (Applied Biosystems). Relative gene expression was quantified by real-time PCR against

the house keeping gene GAPDH using molecular probes (Applied Biosystems) or primers pairs with a product size of around 150 bp. Primers were designed using Primer3web version 4.0.0 and synthetized by Fasmac Bioanalytical Services (Japan).

2.6. Lactate dehydrogenase (LDH) assay

LDH activity was performed according to manufacturer's instructions (Thermo Scientific). Briefly, bronchoalveolar lavage (BAL) fluid or culture supernatant was incubated for 30 min in the dark with an equal volume of the reaction mixture (Substrate + Assay buffer) in a 96-well plate. Dual absorbance was measured according to the manufacturer's instructions.

2.7. Pharmacological inhibitions

The caspase-1-specific inhibitor Ac-YVAD-cmk (Invivogen) and IL-1 receptor antagonist IL1RA, also called Anakinra (MyBioSource) was administered several times before intranasal administration of rb-dsRNA or PBS. Briefly, mice received an intraperitoneal injection (10 mg/kg) of Ac-YVAD-cmk, IL1RA or vehicle twice 12 h apart (for Ac-YVAD-cmk) or 8 h apart (for IL1RA), 12 h (for Ac-YVAD-cmk) or 8 h (for IL1RA) before administration of the first rb-dsRNA dose. These treatment regimens were optimized according to manufacturer's instruction for Ac-YVAD-cmk and as previously described for IL1RA[35, 36, 37].

2.8. Harvesting of lung cells and flow cytometry

Lungs were excised, washed, incubated and homogenized in 5 ml buffer containing collagenase and DNase I. The lung homogenate was passed through a

70 µm cell strainer and centrifuged at 300 x g and re-suspended in the appropriate buffer for antibody staining as follows. Cells were incubated for 30 min with purified rat anti-mouse CD16/CD32 clone 2.4G2 (BD Biosciences) to block non-specific binding before cell-type specific antibodies were applied. For intracellular stain, cells were permeabilized before antibody application. Cells were washed three times and re-suspended with the appropriate buffer before analysis.

2.9. Immunohistochemistry

Excised lungs were fixed in 4% PFA, and dehydrated in sucrose before being frozen in Tissue-Tek® cryomold (Sakura Finetek). Sections were cut and stained as follows. The immuno-blocked sections were incubated with the primary antibody overnight at 4°C before the secondary antibody was applied. The slides were observed under a confocal microscope.

2.10. Statistical analysis

Statistical analysis was performed using Stata 13.1 (StataCorp LP). Two group-comparisons were performed using unpaired two-tailed Student's *t*-tests. Multiple-comparisons were performed using one-way ANOVAs with Bonferroni's tests. Data are expressed as means ± SEM except when otherwise indicated and differences are assessed as ns = not significant, $*p < 0.05$; $**p < 0.01$, or $***p < 0.001$.

Chapter 3

RESULTS

3.1. Rice-bran dsRNA (rb-dsRNA) is potent stimulator of immune response *in vitro* and *in vivo*

Using conventional methods for nucleic acid extraction and purification, rb-dsRNA was purified from Japanese rice Koshihikari cultivar. Rb-dsRNA had a similar size compared to previously reported *Endornavirus* RNA (13.9 kbp)[31, 32]. To confirm the rb-dsRNA identity, the purified nucleic acid was digested with a range of nucleases (Figure 1). The extracted nucleic acid did not contain any obvious trace DNA or DNA-RNA hybrid regions since it was resistant to DNase I, and was sensitive to RNase III, but resistant to S1 nuclease. RNase III and S1 nuclease enzymes have specific activities against dsRNA and single-stranded nucleic acids, respectively. The purified nucleic acid was sensitive to RNase A treatment at a low salt condition, but relatively resistant at a high salt condition. At low salt concentration RNase A enzymatically digests all species of RNA while at high salt conditions its activity is inclined toward single-stranded RNA specificity. These results confirm that the purified nucleic acid is a long dsRNA molecule.

To assess rb-dsRNA's capacity to stimulate immune responses similar to poly I:C, different cell lines were used. We first assessed the capacity of rb-dsRNA to activate cytosolic virus recognition receptors by transfecting mouse embryonic fibroblast (MEF) with the nucleic acid. IFN-β gene was induced by rb-dsRNA transfection in a concentration-dependent manner (Figure 2A) suggesting an efficient activation of RLRs in the mouse fibroblast model. Incubating rb-dsRNA together with Raw 264.7 cells, a murine macrophage cell line, without transfection

reagent also stimulated IFN-β and IP-10 gene and resulted in the release of these proteins in the culture supernatant (Figure 2B, 2C, 2D and 2E). This suggested that rb-dsRNA also reliably stimulates the membrane-bound toll-like receptor 3 (TLR3) in addition to RLRs stimulation.

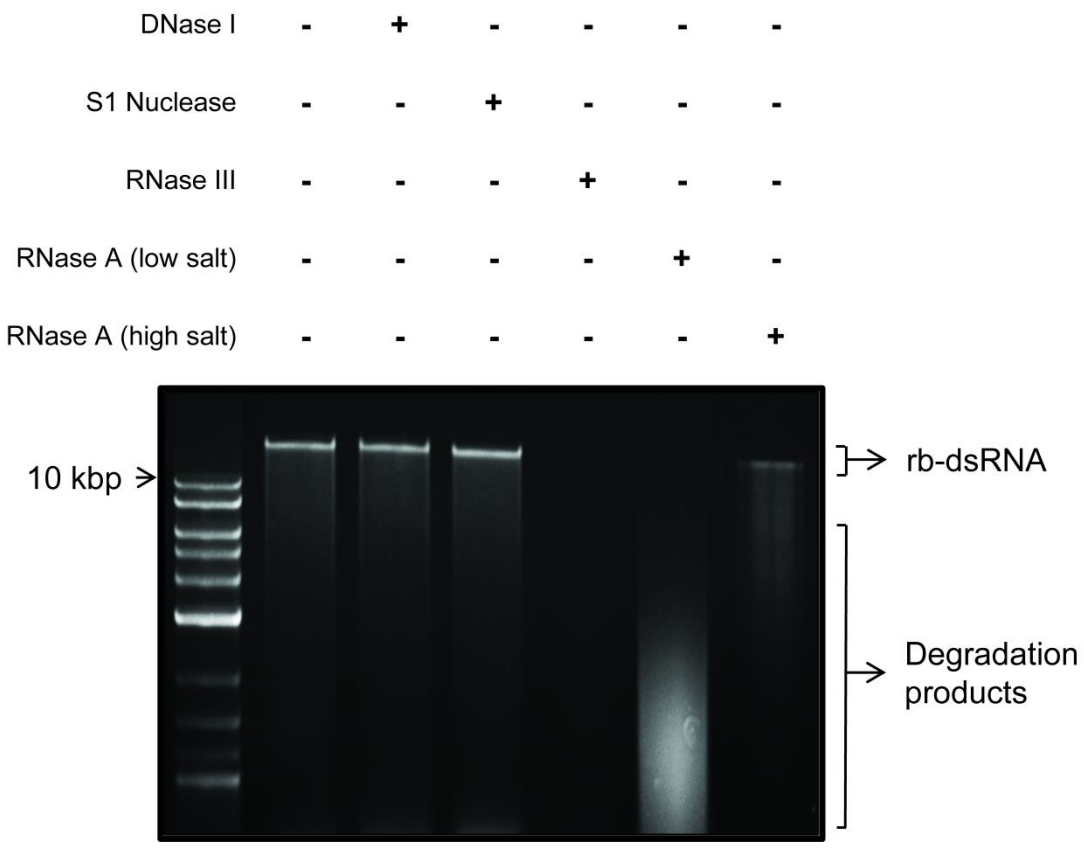

Figure 1. Double-stranded nature of a plant-derived RNA molecule termed rb-dsRNA

Electrophoresis profile of rb-dsRNA on a 0.7% agarose gel. Rb-dsRNA was subjected to DNase I (2 U/µg), S1 nuclease (10 U/µg), RNase III (2 U/µg), RNase A (5 µg/µg) at low salt concentration (0 mM NaCl) and at high salt concentration (0.5 M NaCl) overnight at 37°C. Digested products were then electrophoresed on a 0.7% agarose gel alongside a DNA ladder marker). This data is representative of at least three independent experiments with similar results.

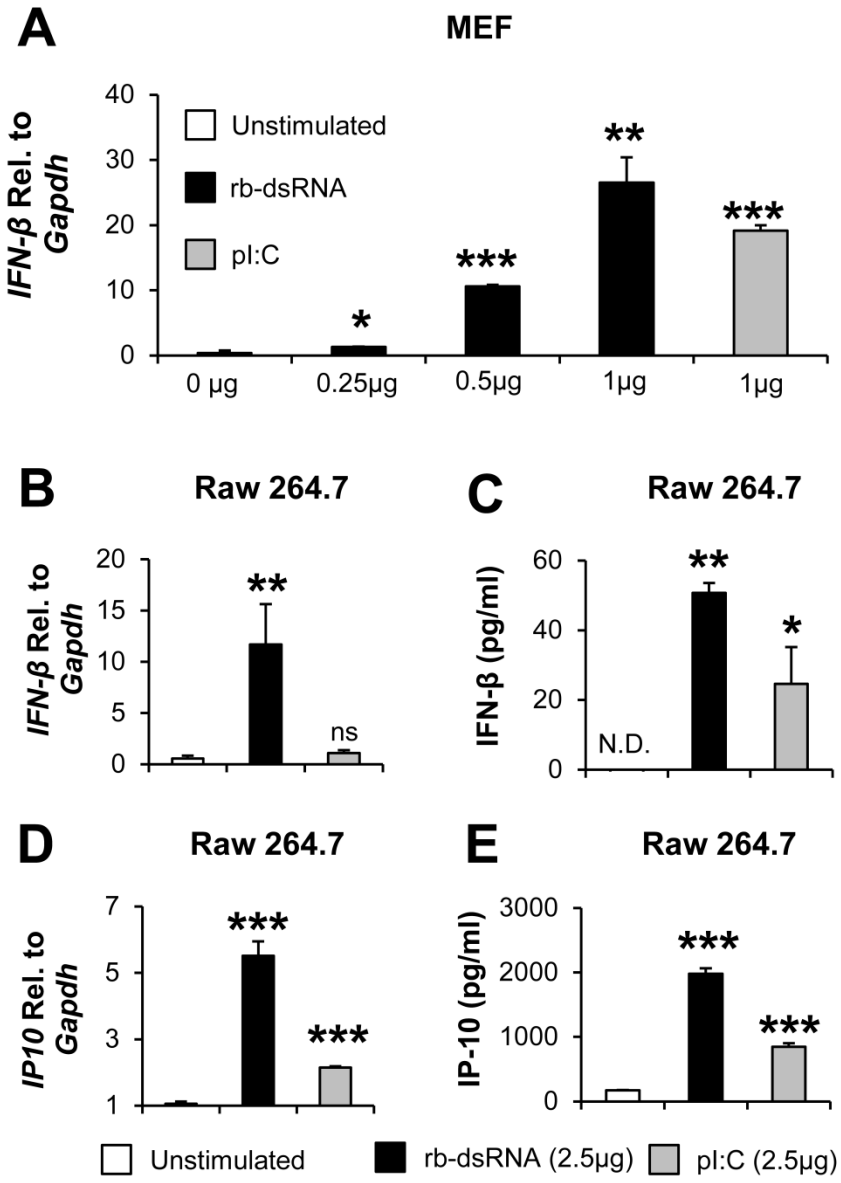

Figure 2. *In vitro* immunostimulatory capacity of rb-dsRNA

(**A**) Primary mice embryonic fibroblasts were transfected using lipofectamine with increasing amount of rb-dsRNA (0.25, 0.5, and 1 µg) and poly I:C (pI:C) as control. (**B to E**) Raw 264.7 cells were incubated with rb-dsRNA or poly I:C (2.5 µg/ml) for 18 hrs. mRNA and protein production were quantified by RT-qPCR and ELISA for IFN-β (**B and C**) and IP-10 (**D-E**). Results are shown as mean ± SEM (*n = 3*) and are representative of at least three independent experiments with similar results. Statistical significance was determined by one-way ANOVA with Bonferroni's test (N.D. = none detected, ns = not significant, **p* < 0.05, ***p* < 0.01, ****p* < 0.001).

To confirm rb-dsRNA capacity to activate both RLRs and TLRs signaling pathways, murine macrophages differentiated from bone-marrow were used. It is now strongly established that MDA5 preferentially senses long dsRNA ligands, while RIG-I recognizes shorter RNAs with different signatures[38, 39]. Keeping that in mind, bone marrow-derived macrophages (BM-MΦ) isolated from wild-type (C57BL/6J), TRIF KO, MDA5 KO and TRIF/MDA5 DKO were stimulated with rb-dsRNA or poly I:C. IFN-β production was not detected in TRIF KO cells, while MDA5 KO partially impaired the induction, and DKO cells did not respond to these dsRNA, suggesting a dominant contribution of the TLR3-TRIF signaling axis for IFN-β gene induction in these cells (Figure 3A). IP-10 production was attenuated in TRIF or MDA5 KO macrophages; however, DKO macrophages hardly responded to rb-dsRNA or poly I:C (Figure 3B). As expected, the results from IFN-β and IP-10 ELISA suggest that rb-dsRNA activates both the membrane-bound TLR3 through TRIF and the cytosolic MDA5.

Furthermore, the involvement of RIG-I in rb-dsRNA-induced immune response was investigated (Figure 3C). Using MEF cells, it was confirmed that rb-dsRNA does not activate RIG-I as indicated by the unchanged induction of IFN-β and MDA5 genes in RIG-I KO MEF. Cells deficient in MDA5, however, lost their ability to activate IFN-β and representative ISGs, MDA5 and RIG-I. This observation suggests that cytosolic rb-dsRNA activates MDA5 with no evidence of RIG-I activation.

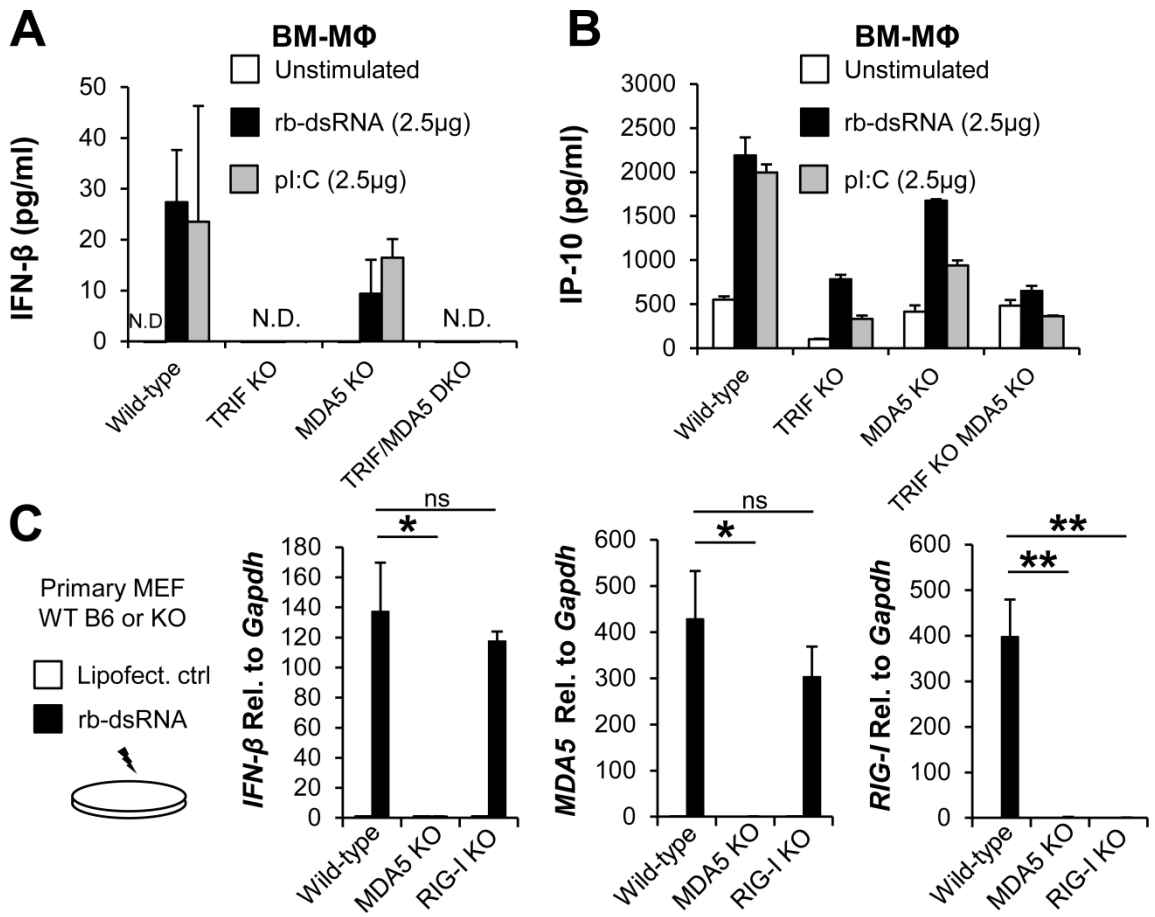

Figure 3. Rb-dsRNA stimulates both TLR3/TRIF and MDA5/IPS-1 axis but not RIG-I *in-vitro*

Bone-marrow derived macrophages (BM-MΦ) from WT, TRIF KO, MDA5 KO and TRIF/MDA5 DKO mice were incubated with rb-dsRNA or poly I:C (2.5 µg/ml) for 18 hrs. Media was analyzed for (**A**) IFN-β and (**B**) IP-10 production by ELISA. (**C**) Mouse embryonic fibroblasts from WT, MDA5 KO and RIG-I KO mice were transfected with rb-dsRNA (1 µg) and incubated for 18 hrs. IFN-β, MDA5 and RIG-I induction was quantified by qRT-PCR. Mean ± SEM (*n* = *3*) of at least two independent experiments with similar results. Statistical significance was determined by unpaired student *t-test* and one-way ANOVA with Bonferroni's test (N.D. = none detected, ns = not significant, **p* < 0.05, ***p* < 0.01, ****p* < 0.001).

In vivo assessment of rb-dsRNA was performed to investigate its physiological relevance as an immune stimulator. Intranasal (i.n.) administration of rb-dsRNA in mice resulted in induction of antiviral cytokine and chemokine genes.

Most notably, mRNA levels of IFN-β and IFN-α4 (Figure 4A), members of the type-I interferon family, were up-regulated very quickly, reaching a peak of expression at around 8 hrs. Several other interferon-stimulated genes were also up-regulated. Expression of BST2 (also known as tetherin) (Figure 4A), a host factor blocking the release of newly formed enveloped viruses[40], was gradually increased. Expression of interferon-stimulated genes reported to inhibit virus entry, replication, and maturation were also notably increased with different kinetics (Figure 4B). Interferon-induced transmembrane protein-3 (IFITM3) is known to inhibit entry and replication of IAV and several other viruses[41, 42]; ISG56 is known to inhibit replication and translation of several viruses[41, 43, 44]; Pai-1 inhibits extracellular maturation of IAV [45]. Elevated expression of chemo-attractants with C-X-C-motifs (NAP-3, MIP-2α, and IP-10) suggested that rb-dsRNA can provoke leukocyte recruitment (Figure 4C). Expression levels of inflammatory cytokines, such as IL-1β, IL-6, and TNF-α (Figure 4D), were transiently increased, suggesting activation of inflammatory reactions. Taken together, the i.n. administration of rb-dsRNA mimicked virus-derived dsRNA by quickly up-regulating the expression of a wide range of cytokines and chemokines associated with immune responses.

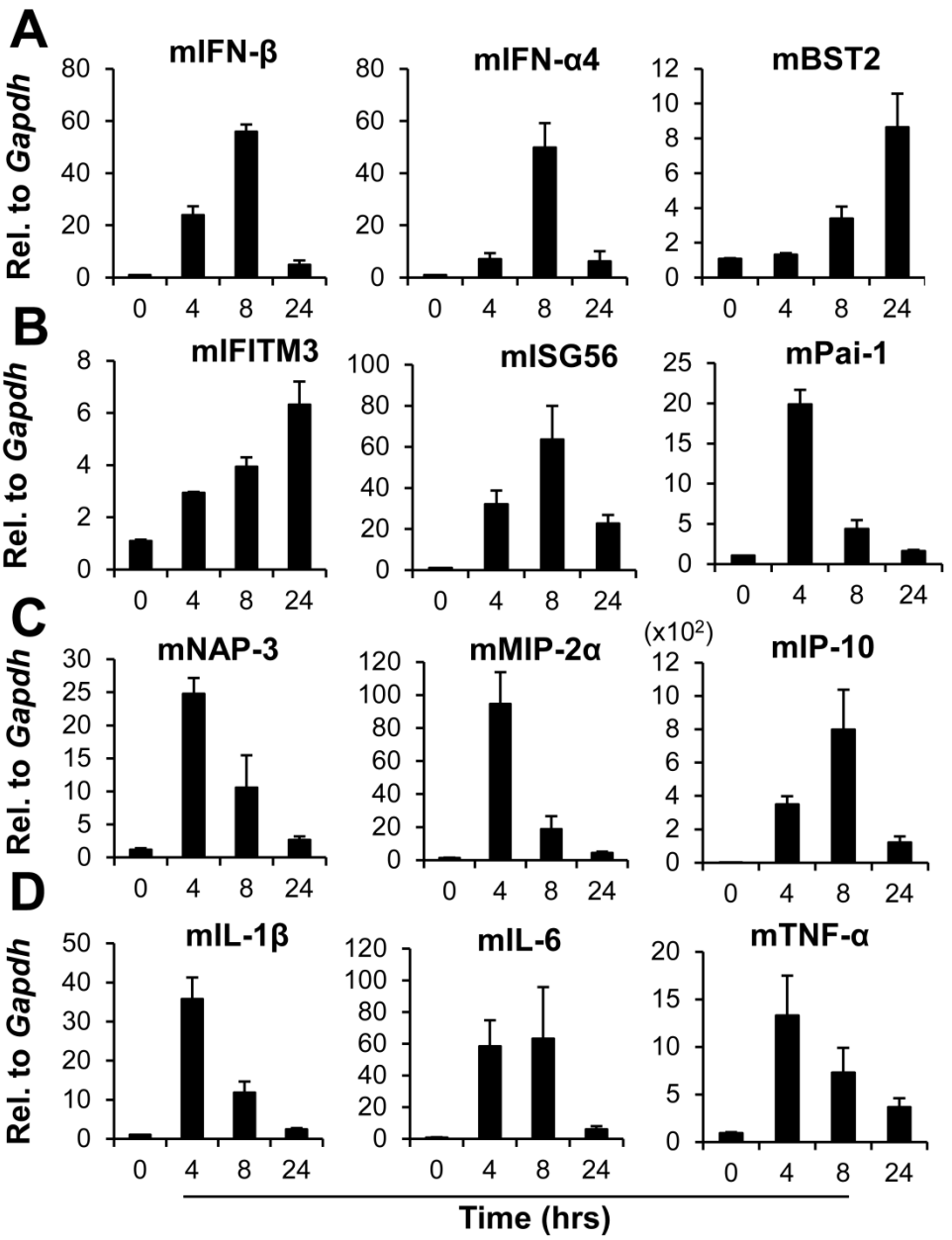

Figure 4. Intranasal administration (i.n.) of rb-dsRNA reliably stimulates several genes of innate immunity in murine lungs

Wild-type mice (B6) were administered (i.n.) with rb-dsRNA or PBS as negative control. Lungs were harvested at indicated time points and expression of selected genes involved in innate immunity was analyzed by qRT-PCR. Genes are grouped as (**A** and **B**) IFN-I and interferon-stimulated genes, (**C**) chemokines and (**D**) inflammatory cytokines. Results are shown as mean ± SEM (*n = 3*) and are representative of at least two independent experiments with comparable results.

3.2. Rb-dsRNA activates TRIF and IPS-1 signaling through TLR3 and MDA5 in alveolar macrophages in the respiratory tract

To investigate the activation of signaling pathways, knockout mouse models were used, as depicted in Figure 5A. At 8 hrs and 12 hrs after i.n. rb-dsRNA administration, mice were analyzed for mRNA expression and protein secretion, respectively. These time points corresponded to the mRNA (Figure 4) and protein peaks (data not shown) of IFN-I and most cytokines tested. Mice lacking IPS-1 and MDA5 showed similar IFN-β induction (Figure 5B). These expression levels, however, were significantly lower than those in wild-type mice suggesting that rb-dsRNA was sensed by MDA5 and triggered signaling through IPS-1 in murine lungs. On the other hand, mice lacking TRIF, the adaptor molecule for TLR3 signaling, also exhibited reduced IFN-β expression, suggesting the involvement of TLR3 *in vivo*. To further confirm the involvement of both IPS-1 and TRIF signaling pathways, mice lacking both TRIF and MDA5 (TRIF/MDA5 DKO) were i.n. administered with rb-dsRNA. Up-regulation of IFN-β mRNA and protein in bronchoalveolar fluid (BALF) was completely abolished in DKO mice (Figure 5C and Figure 5D). Consistent with these results, rb-dsRNA-induced expression of IP-10 was also abrogated in DKO mice (Figure 5E). In line with *in vitro* observations, these *in vivo* results propose that rb-dsRNA is recognized by both TLR3 and MDA5, and subsequently induces IFN production through TRIF and IPS-1 adaptors, respectively.

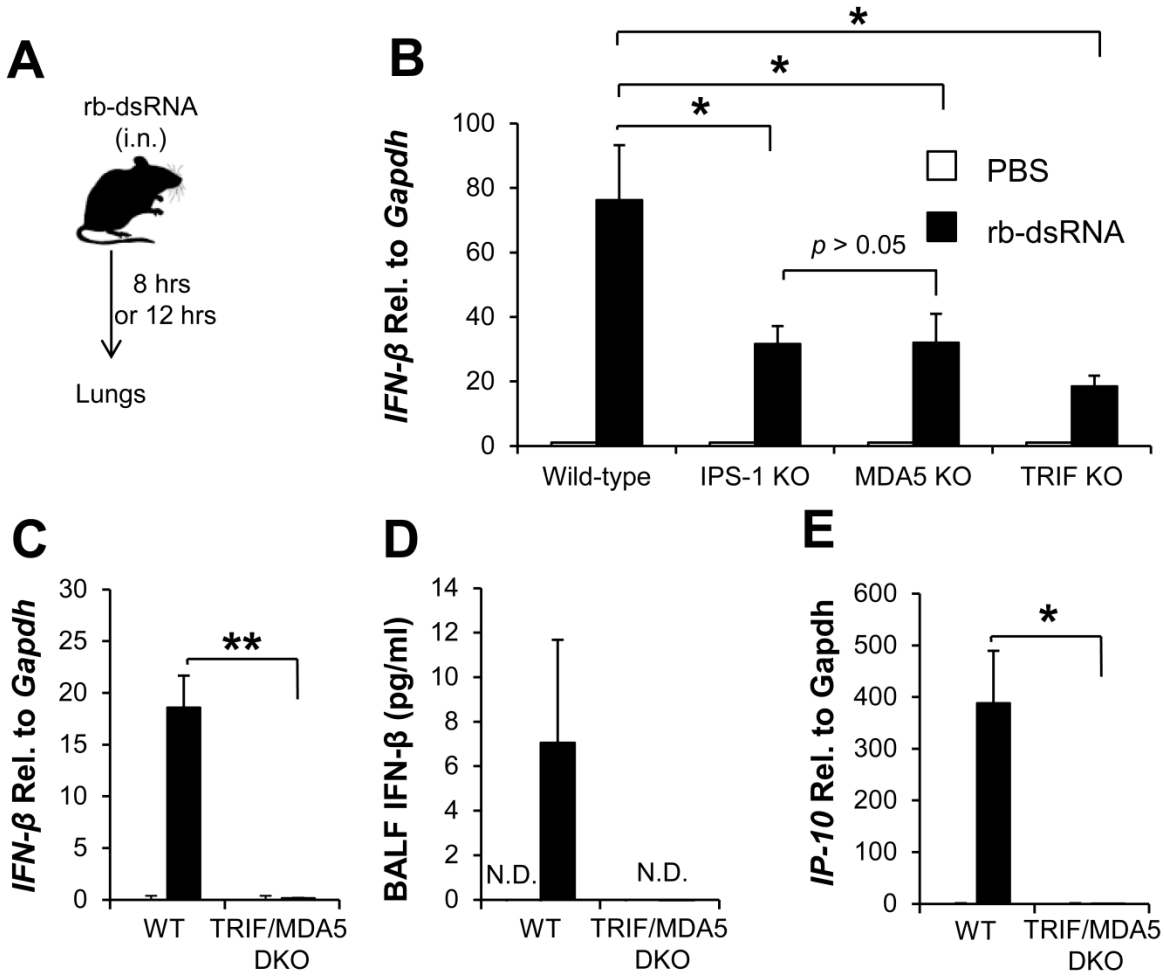

Figure 5. Rb-dsRNA stimulates both TLR3/TRIF and MDA5/IPS-1 signaling *in-vivo*

(**A-E**) Wild-type B6 and KO mice were administered (i.n.) with rb-dsRNA or PBS. (**A**) Schematic representation of experimental design. (**B**) Wild-type, IPS-1 KO, MDA5 KO and TRIF KO mice were administered with rb-dsRNA or PBS and lungs were harvested 8 hrs later for qRT-PCR analysis of IFN-β (*n = 6 to 8*). (**C**) Wild-type and TRIF/MDA5 DKO mice were administered rb-dsRNA or PBS and lungs harvested 8 hrs post-administration for qRT-PCR analysis and (**D**) 12 hrs for ELISA of IFN-β. (**E**) Quantitative RT-PCR analysis of IP-10 in murine lungs. Results are shown as mean ± SEM (*n = 4 to 6*). Results are representative of at least two independent experiments with similar results. Statistical significance was determined by unpaired student *t-test* and one-way ANOVA with Bonferroni's test (N.D. = none detected, ns = not significant, **p* < 0.05, ***p* < 0.01).

At the cellular level, these results were in line with the BM-MΦ stimulation experiment (Figure 3) and suggested the possible implication of macrophages in the activation of immune response by rb-dsRNA in murine lungs. Cells mainly responsible for rb-dsRNA-induced IFN-I in the lungs were investigated. Based on the previous data, it was speculated that this response is mediated by phagocytic cells in the lungs. Macrophage populations are considered professional phagocytes constantly present in tissues as guards against foreign invasion. Macrophages, particularly alveolar macrophages (AMΦ), have been shown to act as sentinels for tissue homeostasis by driving virus-induced and RNA-induced IFN-I production in the lungs. By doing so, they act as primary activators of innate immunity in the lungs[9, 46]. To identify cells producing IFN-I upon i.n. rb-dsRNA administration, the two macrophage populations in the lung were discriminated: the interstitial macrophages (IMΦ), located in the parenchymal space, and the AMΦ, found in the airway space[47, 48]. SiglecF^{+} F4/80^{+} (AMΦ) and SiglecF^{-} F4/80^{+} (IMΦ) macrophages were isolated by magnetic-activated cell sorting. Quantitative PCR revealed that AMΦ was the main lung macrophage population exhibiting up-regulation of IFN-I upon administration of rb-dsRNA (Figure 6A and 6B).

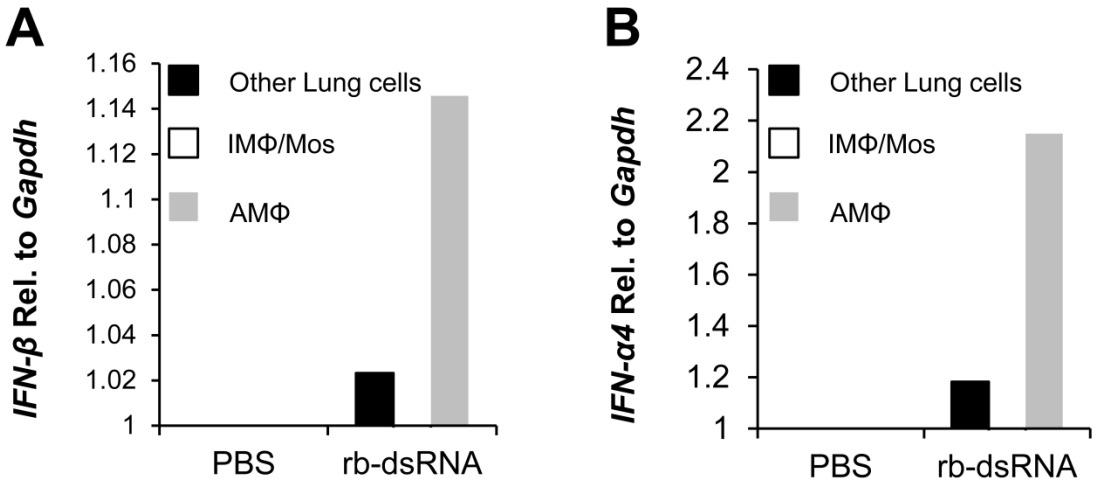

Figure 6. Rb-dsRNA mainly stimulates alveolar macrophages

Cells obtained from digested lungs of five wild-type B6 mice were separated by magnetic-activated cell sorting (MACS) for the collection of alveolar macrophages (AMΦ) as SiglecF^{+} F4/80^{+}, interstitial macrophages (IMΦ) or monocytes (Mos) as SiglecF^{-} F4/80^{+} or other cell types as SiglecF^{-} F4/80^{-}. (**A**)The sorted cells were analyzed by qRT-PCR for the expression of IFN-β and (**B**) IFN-α4. Results are representative of at least two independent experiments with similar results.

Furthermore, taking advantage of their strategic localization, a depletion experiment to directly assess the contribution of AMΦ to IFN-I and cytokine expression was performed. Macrophage depletion by intranasal administration of clodronate liposome resulted in depletion of AMΦ with no obvious reduction in the percentage of SiglecF^{-} F4/80^{+} (IMΦ/Monocytes) (Figure 7A). In fact, IMΦ/Monocytes were increased presumably as a result of monocyte infiltration in response to macrophage depletion. Depletion of AMΦ significantly reduced rb-dsRNA-induced IFN-I (Figure 7B) and the IFN-I-stimulated gene IP-10 (Figure 7C). These data suggest that lung macrophages are the major source of IFN-I induced

by rb-dsRNA, and that the macrophage sub-population responsible for IFN-I production is AMΦ.

Taken together, these observations clearly indicate that rb-dsRNA is potent activator of both MDA5/IPS-1 and TLR3/TRIF signaling axis both *in vitro* and *in vivo.* In the respiratory tract (lungs), alveolar macrophages are the main population up taking rb-dsRNA upon i.n. administration and producing IFN-I as a key initiating step to the activation of immune response.

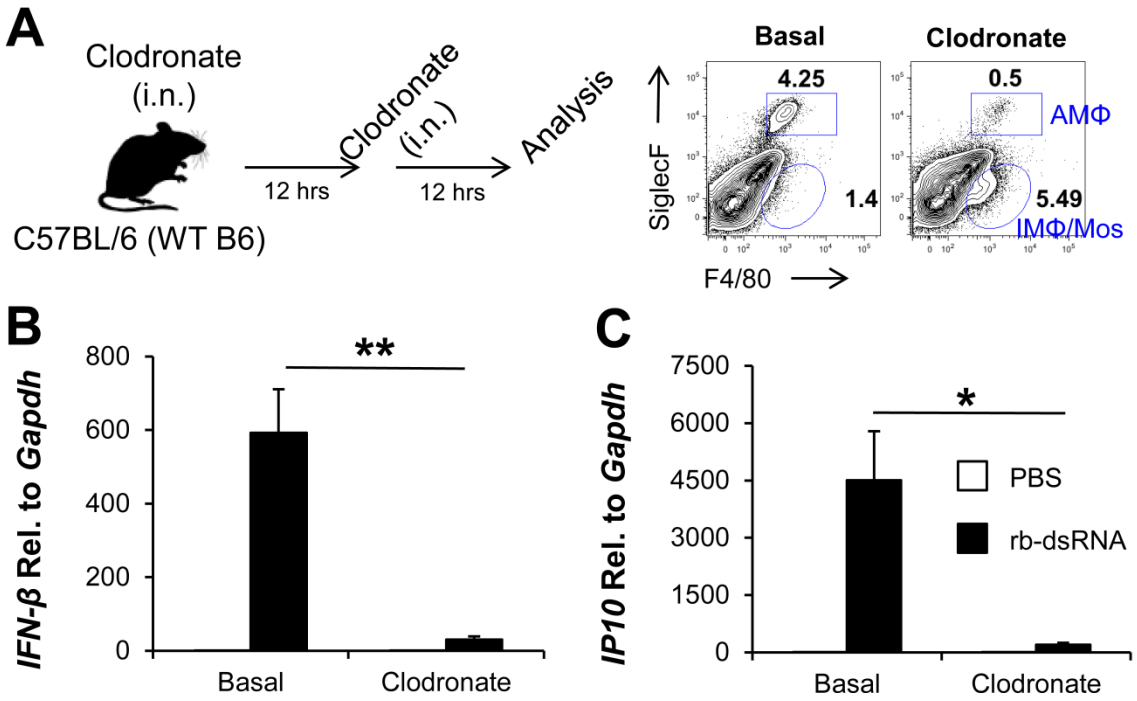

Figure 7. Alveolar macrophages are the main producers of IFN-I after i.n. rb-dsRNA

(**A**) Schematic representation of macrophage depletion using clodronate liposome. (**B**) After alveolar macrophage depletion as depicted in (**A**), rb-dsRNA was i.n. administered and lungs harvested 8hrs later. Cytokine expressions were quantified by RT-qPCR. Results are representative of at least two independent experiments with similar results. Statistical significance was determined by unpaired student *t-test* and one-way ANOVA with Bonferroni's test (*$p < 0.05$, **$p < 0.01$).

3.3. Intranasal rb-dsRNA enhances antiviral immunity against respiratory viruses

Since rb-dsRNA activates a cascade of events associated with the innate immune response in the lung, its ability to induce immune protection against respiratory viruses (IAV H1N1 Puerto Rico/8/34 and Sendai virus) was assessed. Mice were i.n. administered with rb-dsRNA before (Figure 8A) or after (Figure 8B) the IAV challenges to respectively assess its prophylactic and therapeutics potential. Although both treatment regiments demonstrated rb-dsRNA capacity to stem virus proliferation in the lungs, they failed to significantly improve host survival (data not shown). To overcome this difficulty, mice were treated twice (before and after) throughout this study, as depicted in Figure 9A, to characterized the antiviral activity induced by rb-dsRNA. The combined regiment showed significantly higher protective capacity overall, reducing mortality induced by IAV (Figure 9B) and Sendai virus-induced morbidity (Figure 9C). Mice treated with rb-dsRNA exhibited significantly higher survival upon IAV infection. IAV is known to cause lung injury which can culminate in hypoxia, respiratory failure, and death[26, 49, 50, 51, 52]. Treatment with rb-dsRNA reduced IAV-induced acute inflammation, which was correlated with a higher lung/body weight ratio (Figure 10A and Figure 10B).

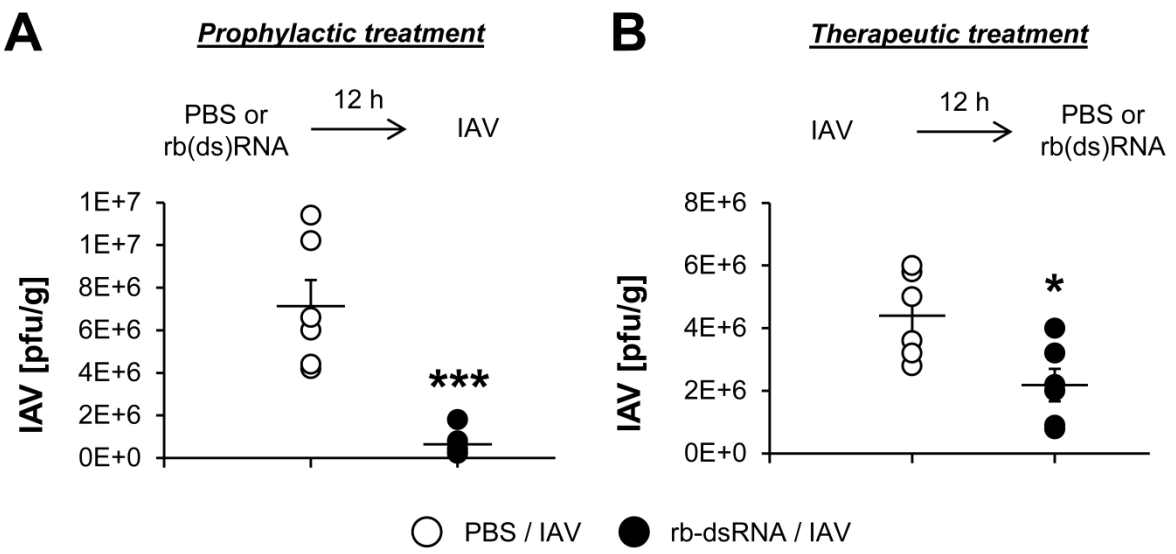

Figure 8. Rb-dsRNA reduces IAV virus load in the lungs

(**A**) B6 WT mice were i.n. with rb-dsRNA 12 hours before being infected with 10^3 pfu of IAV. Lungs were harvested 24 hours post-infection and analyzed (**B**) B6 mice were infected with IAV as described in (**A**) before being i.n. administered rb-dsRNA. Lungs were analyzed 24 hours post-infection by plaque assay. Results are representative of at least two independent experiments with similar results. Statistical significance was determined by unpaired student *t-test* (*$p < 0.05$, ***$p < 0.001$).

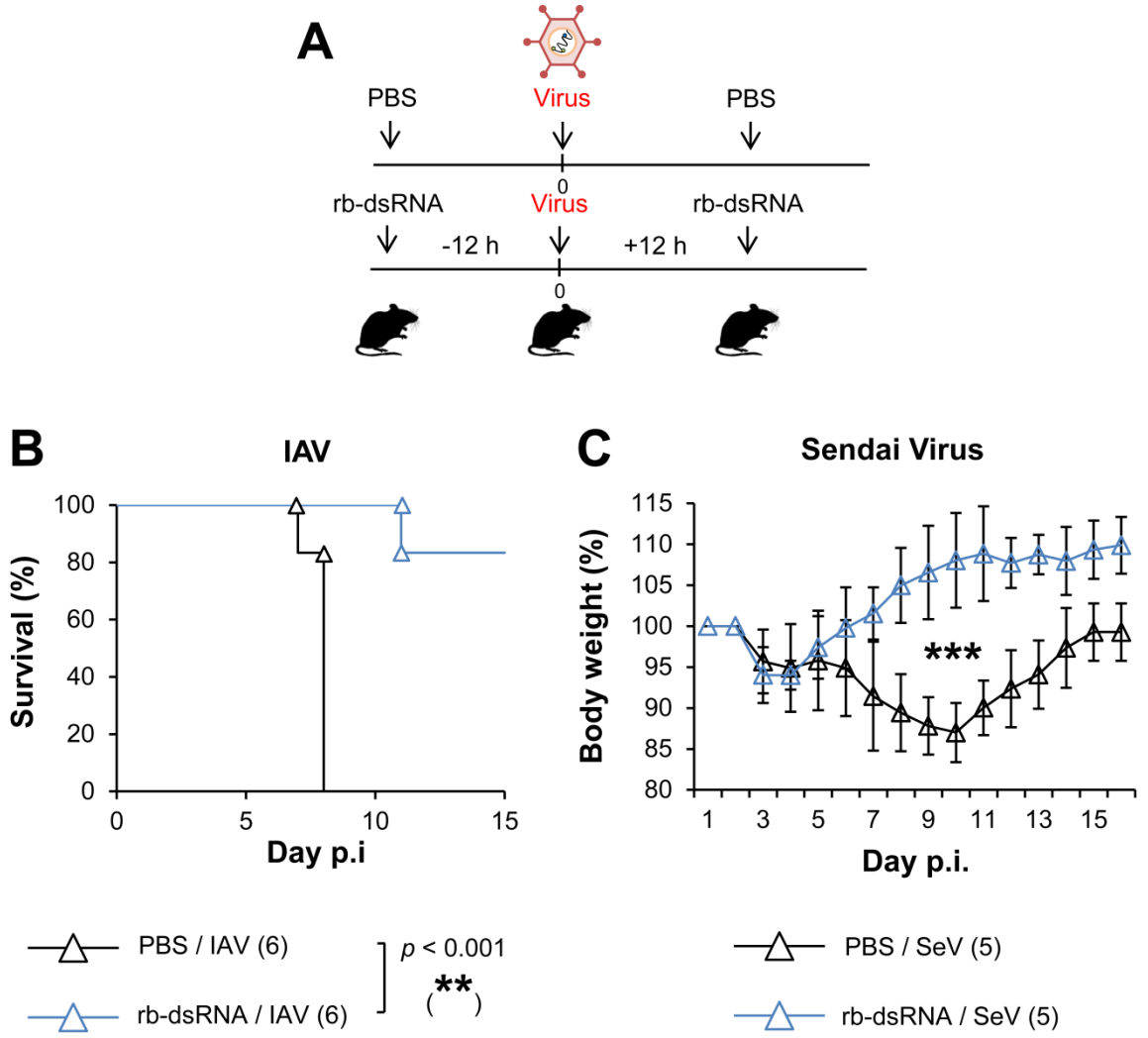

Figure 9. Rb-dsRNA reduces mortality and morbidity caused by respiratory viruses

Wild-type (B6) mice were treated (i.n.) with rb-dsRNA prio- and post-infection with lethal amount respiratory viruses as depicted in (**A**). (**B**) Survival rate of mice infected with IAV and treated with rb-dsRNA compared to untreated infected mice (*n* = *6*). (**C**) Body weight of B6 mice infected with Sendai virus (SeV) Cantell strain and treated or not as depicted in (**A**). Body weight was monitored once a day and shown as body weight compared to initial weight. Results are representatives of at least two independent experiments with comparable results. Statistical significance was determined by unpaired student *t-test* (**$p < 0.01$, ***$p < 0.001$).

Next, IAV titer in the lung was examined (Figure 11A). Rb-dsRNA treatment, as depicted in Figure 9A, reduced IAV titer at 1 and 3 days p.i.; however, at 7 days p.i., the infectious viral titer declined and the difference was indistinguishable between treated and untreated animals. Similarly, viral RNA quantification showed suppressed viral replication at 1 and 3 days p.i., but not at 7 days p.i. (Figure 11B). Inhibition of IAV replication at early time points was also apparent in histochemical analysis of lung tissues samples (Figure 11C). The number of IAV antigen-positive cells was clearly reduced at 1 day p.i. in rb-dsRNA-treated mouse, while this change was less obvious at 7 days p.i. Interestingly, SeV-infected mice exhibited sustained inhibition of viral replication up to 7 days p.i. (Figure 11D). These results suggest that treatment with rb-dsRNA enhanced antiviral immunity and reduced viral load in the lungs early in infection thereby protecting the host from acute lung injury, respiratory failure and death.

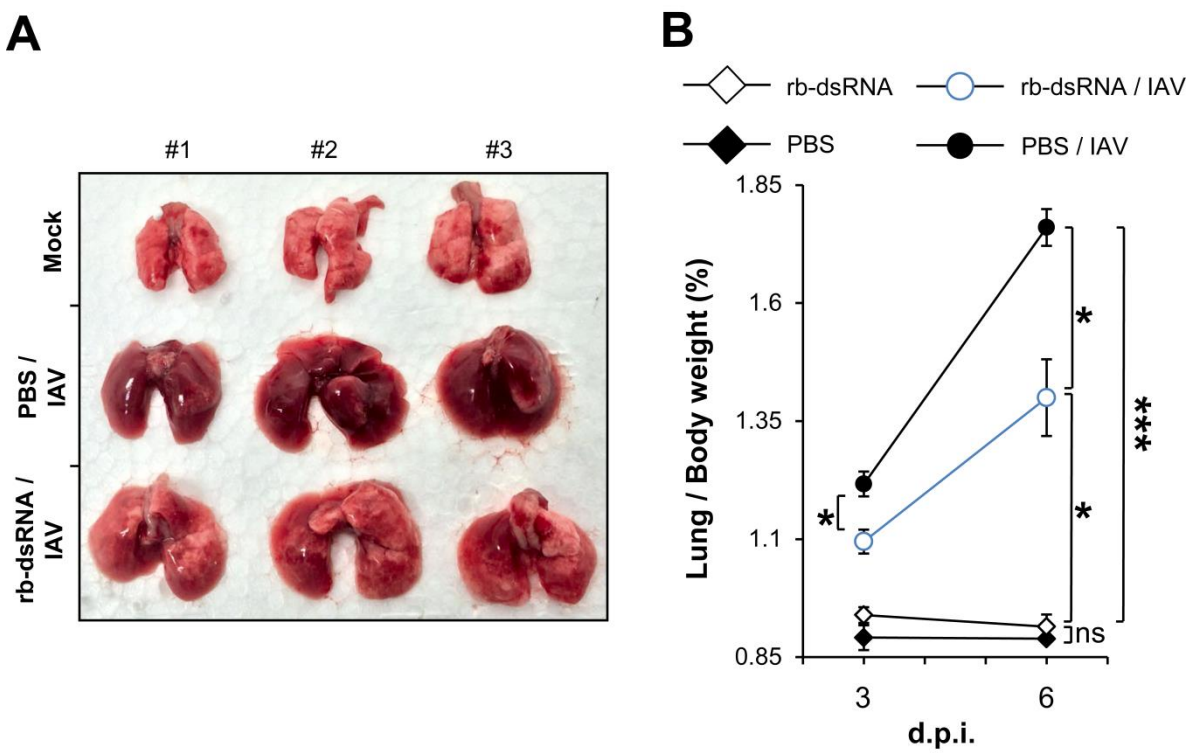

Figure 10. Rb-dsRNA reduces mortality and morbidity caused by respiratory viruses

Wild-type (B6) mice were treated (i.n.) with rb-dsRNA prio- and post-infection with lethal amount IAV. (**A**) A representative image of lungs harvested 7 dpi with 500 pfu of IAV. (**B**) Wild-type mice were infected and treated or left untreated as indicated. Lungs harvested 3 and 6 dpi were snap-frozen with liquid nitrogen to remove water and weighed. Lung weight to body weight ratio was used to assess the severity of virus-induced pathology. Results are shown as mean ± SEM (*n* = *3*) and are all representatives of at least two independent experiments with comparable results. Statistical significance was determined by unpaired student *t-test* and one-way ANOVA with Bonferroni's test (ns = not significant, **p* < 0.05, ***p* < 0.01, ****p* < 0.001).

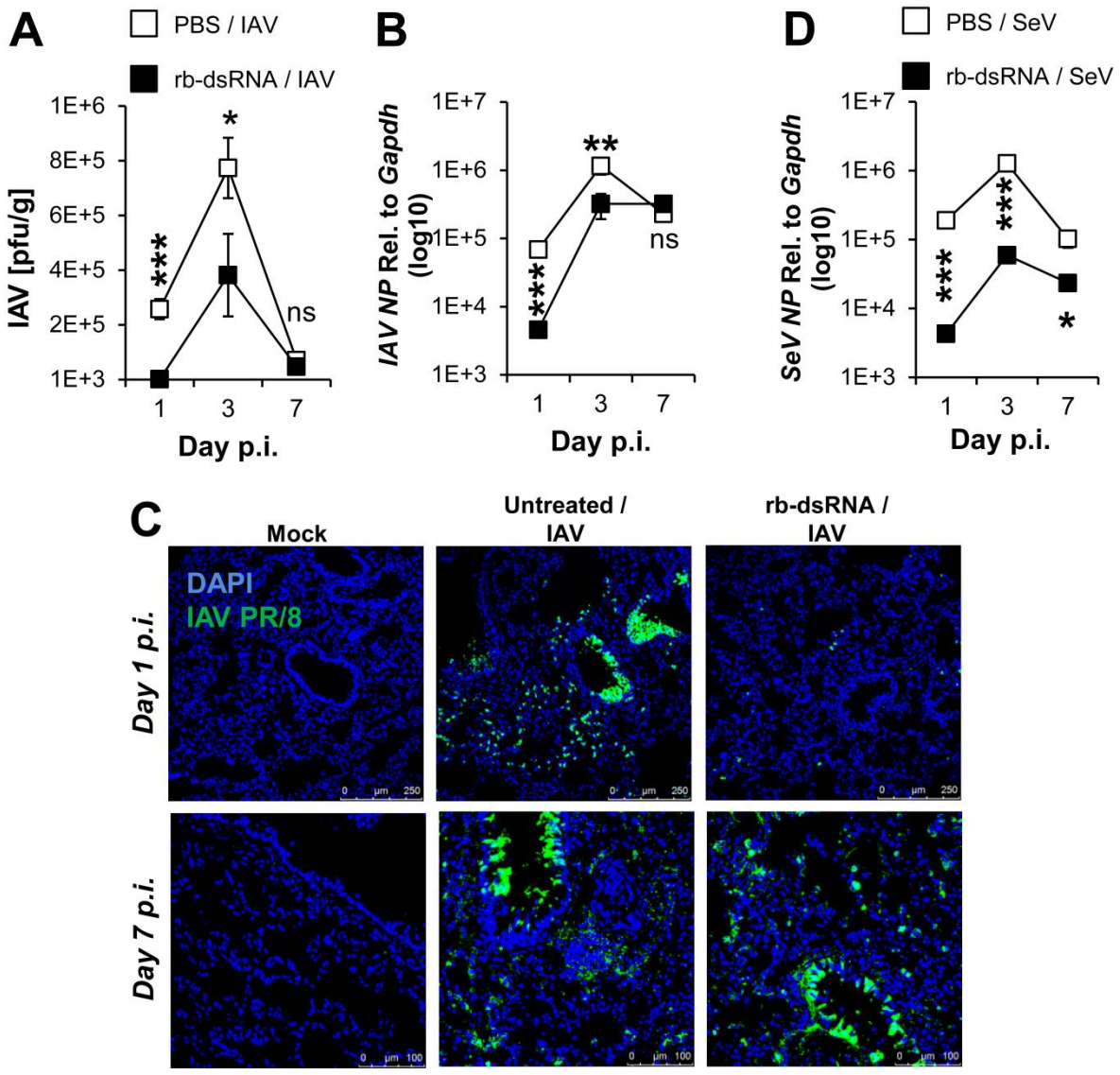

Figure 11. Rb-dsRNA reduces virus burden in the lungs

Wild-type (B6) mice infected with lethal dose of IAV (*n = 4 to 6*). Lungs harvested 1, 3 and 7 dpi were subjected to (**A**) plaque assay and (**B**) qRT-PCR. (**C**) Representative images of immunohistochemistry of frozen lung sections at 24 hpi (scale bare: 250µm) and 7 days p.i. (scale bar: 100µm) with IAV. A polyclonal antibody recognizing whole virus was used. (**D**) Wild-type mice (B6) were infected with SeV; virus replication was quantified by qRT-PCR analysis of the NP gene 1, 3 and 7 dpi (*n = 3 to 4*). Results are shown as mean ± SEM. Results are representative of at least three independent experiments with similar results. Statistical significance was determined by one-way ANOVA with Bonferroni's test (ns = not significant, *$p < 0.05$, **$p < 0.01$, ***$p < 0.001$).

3.4. Rb-dsRNA-driven protection involves IFN-I signaling-independent event(s)

To confirm whether rb-dsRNA-driven antiviral protection is directly linked to TLR3/TRIF and MDA5/IPS-1 recognition of the nucleic acid and subsequent IFN production, mice deficient in both TRIF and IPS-1 signaling pathways (TRIF/MDA5 DKO) and the type I IFN receptor (IFNAR1 KO) were tested. Survival was examined in respective mice treated with rb-dsRNA and challenged with IAV. In TRIF/MDA5 DKO mice, rb-dsRNA did not confer resistance to IAV infection in marked contrast to wild-type mice treated with rb-dsRNA (Figure 12A). In contrast, IFNAR1 KO mice exhibited partially reduced protection (Figure 12B). Furthermore, lung tissues of these mice were examined. The inhibitory effect of rb-dsRNA treatment on infectivity and viral accumulation in the lungs was absent in TRIF/MDA5 DKO mice (Figure 13A, 13B, and 13C), suggesting that the inability to sense rb-dsRNA abolished the activation of antiviral protection against IAV. Additionally, TRIF-axis appeared to be dominant compared to IPS-1 (Figure 13B); this was in line with previous observations (Figure 3). Consistent with the survival result (Figure 12B), IFN-I receptor deficiency exhibited partial rb-dsRNA-induced antiviral protection (Figure 13C) while IFN-III (IL28α) signaling did not contribute in the observed antiviral inhibition.

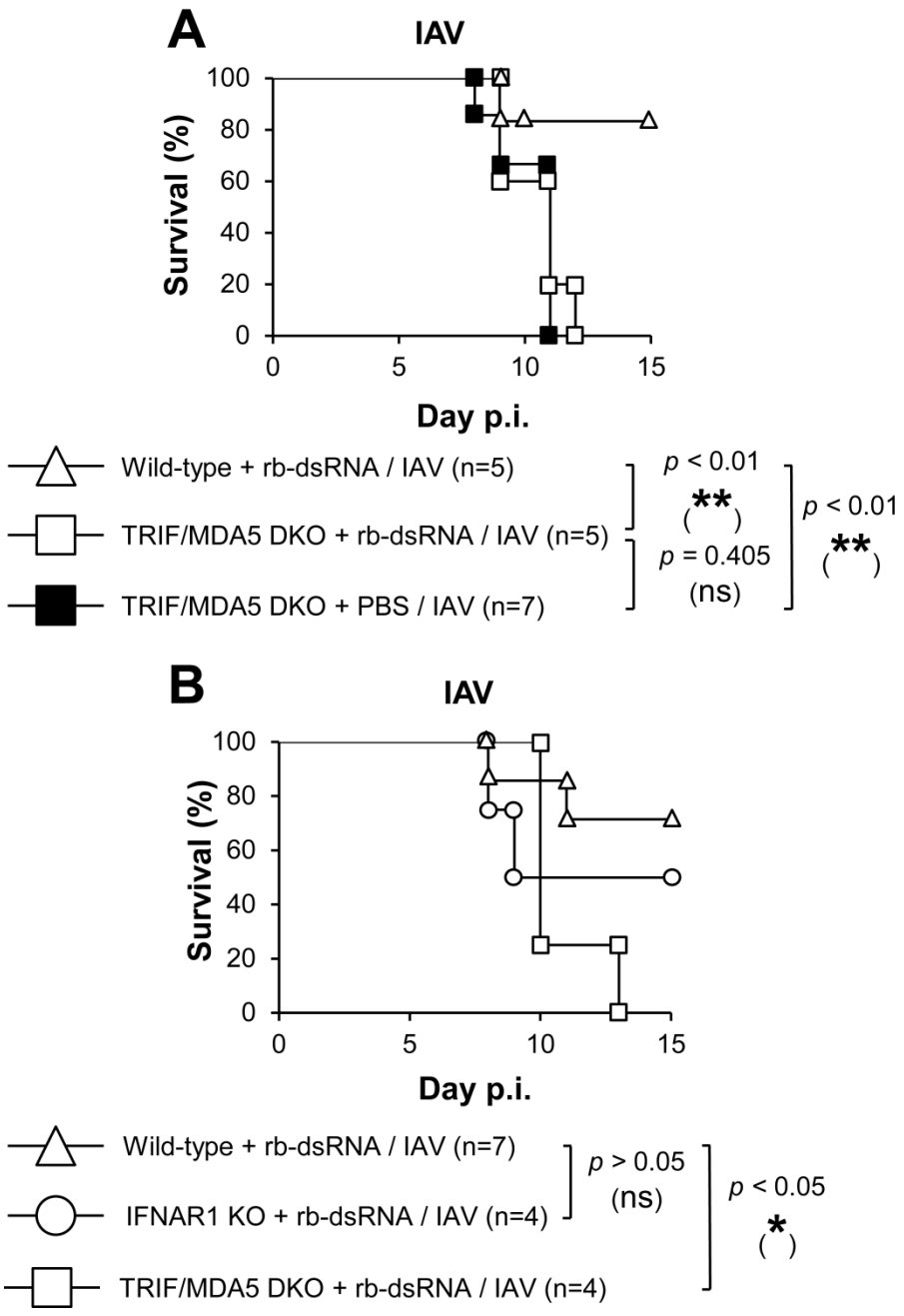

Figure 12. TLR3/TRIF and MDA5/IPS-1 drives decreased mortality of IAV infected mice

(**A**) Wild-type (B6) and TRIF/MDA5 DKO mice infected with lethal dose of IAV and survival rate of untreated and treated mice was monitored. (**B**) Survival rate of B6, TRIF/MDA5 DKO and IFNAR1 KO mice. Results are representative of two independent experiments with comparable results. Statistical significance was determined by one-way ANOVA with Bonferroni's test (ns = not significant, *$p < 0.05$, **$p < 0.01$).

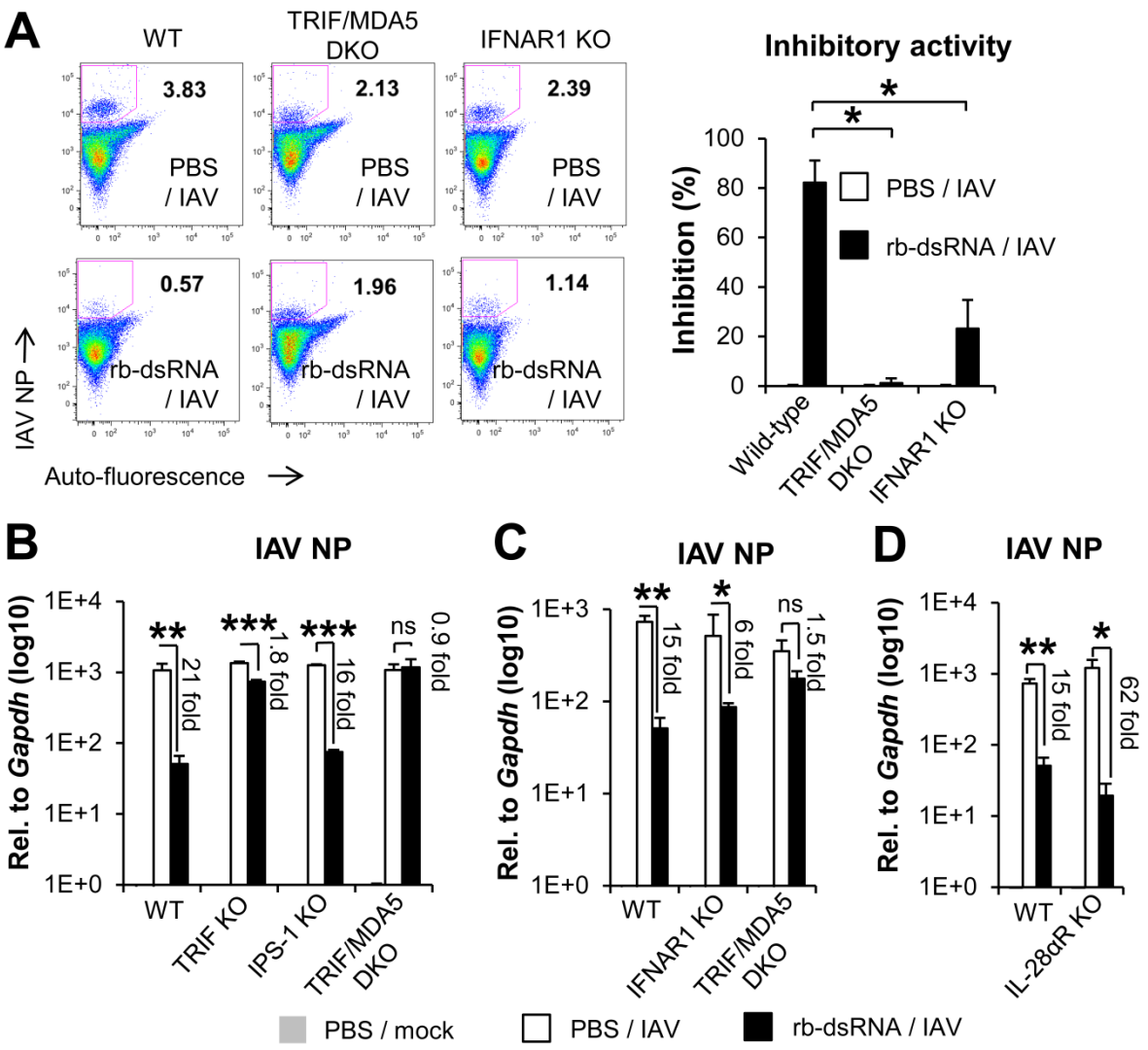

Figure 13. RNA recognition is required for antiviral protection while IFN-I signaling contributes partially

Mice were infected with lethal dose of IAV Puerto Rico/8/34 and treated or not with rb-dsRNA. (**A**) FACS of lung cells from infected WT and KO mice. Cells were stained for IAV NP protein. Percentage inhibition (right): the percentage of NP^+ cells from untreated mice was considered as maximum NP^+ signal within each group. (**B, C and D**) Lung harvested from WT and KO mice were analyzed by qRT-PCR 24 hpi to quantify viral RNA. All Results are shown as mean ± SEM (*n = 3 to 4*) and are representative of at least two independent experiments with similar results. Statistical significance was determined by unpaired student *t-test* and one-way ANOVA with Bonferroni's test (ns = not significant, **p* < 0.05, ***p* < 0.01, ****p* < 0.001).

3.5. Rb-dsRNA modulates immunity by reshaping cellular population in the lungs

To investigate the residual antiviral protection observed in mice deficient in IFNAR1, it was speculated that this IFNAR1-independent inhibition could be related to a cell population change in the lungs. Therefore, the cellular population in the targeted organ was characterized. Leukocytes were enzymatically isolated from the whole lung and monitored according to respective cell markers.

Notably, a dramatic decline of AMΦ frequency was induced after rb-dsRNA treatment within 12 hours. This frequency increased gradually, recovering to the original level after a few days. Lethal IAV infection also induced a decrease of AMΦ, reaching the lowest level after 3 days, without notable recovery up to 6 days. Rb-dsRNA-treated and IAV-infected mice showed a sharp decrease of AMΦ, similar to those treated with rb-dsRNA alone, but unlike IAV-infected mice, the AMΦ number partially recovered up to 6 days without causing its complete depletion (Figure 14A).

In contrast to AMΦ, transient neutrophil accumulation was induced by rb-dsRNA and returned to normal level after 3 days. IAV infection alone induced moderate neutrophil accumulation at 72 h p.i. and kept its level at 144 h p.i. Rb-dsRNA-treated and IAV-infected mice showed a sharp increase of neutrophils, similar to those treated with rb-dsRNA alone, but unlike IAV-infected mice, their number continued to decline until 6 days p.i. (Figure 14B).

Similar to neutrophils, monocyte accumulation was induced by rb-dsRNA and IAV infection in a transient and persistent manner, respectively. Unlike neutrophils, rb-dsRNA-treated and IAV-infected mice exhibited a biphasic increase in monocytes, resulting in a similar monocyte level between untreated and rb-dsRNA-treated and IAV-infected mice at 6 days p.i. (Figure 14C)

These results illustrate that rb-dsRNA treatment and viral infection differentially promoted dynamic immune cell population change in the lungs. Since neutrophils are known to contribute to immune response against IAV[11, 52, 53], it was speculated that rb-dsRNA-driven neutrophil recruitement could contribute to antiviral protection. Mice lacking IFNAR1 recruit less neutrophils in the lungs (Figure 15A), presumably because neutrophil-attracting chemokines are also induced by IFN-I. Keeping that in mind, wild-type and IFNAR1 KO mice were tested. However, depletion of neutrophils using anti-Ly-6G clone 1A8[11, 54], in wild-type and IFNAR1 KO failed to abrogate the residual inhibition of IAV induced by rb-dsRNA (Figure 15B). This suggested that the cause of the observed inhibition was elsewhere. Since AMΦ are key players in immunity in the respiratory tract and a dramatic change in their frequency was observed, this population was investigated more deeply.

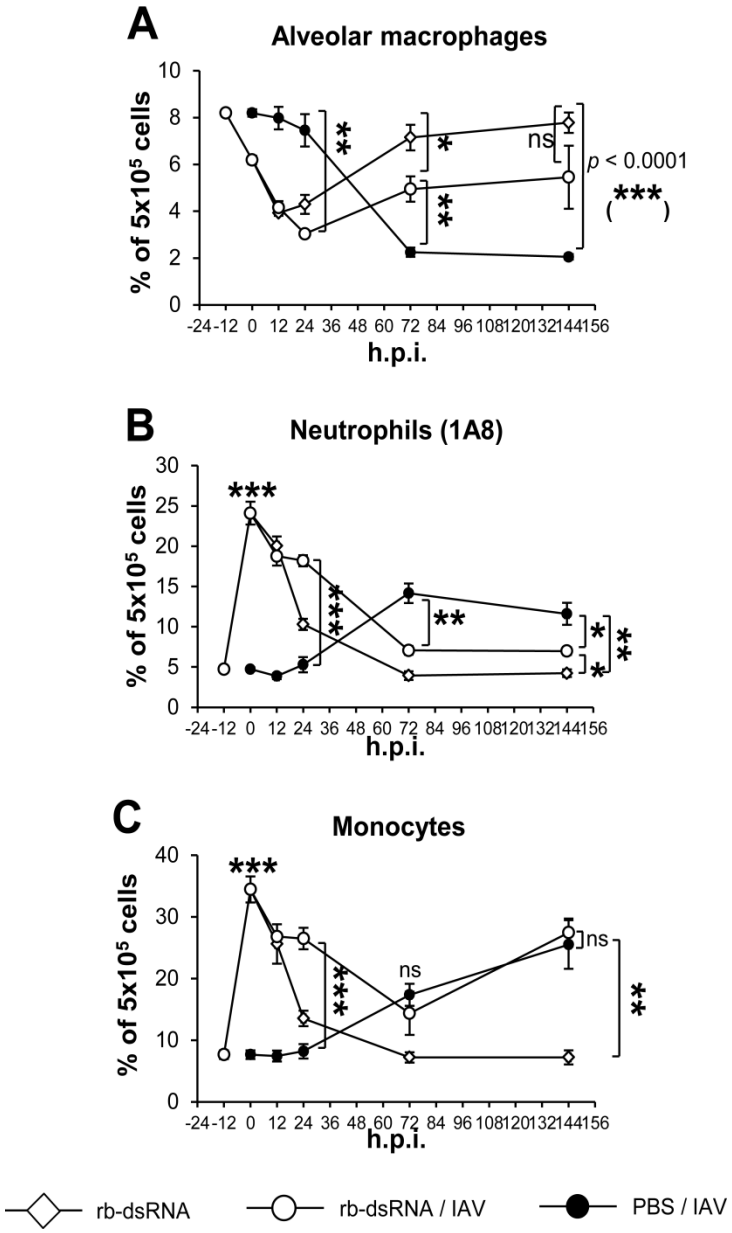

Figure 14. Rb-dsRNA remodels the cellular population in the lungs

Wild-type mice were inoculated with PBS or rb-dsRNA and infected with IAV or left uninfected. Lungs harvested at -12, 0, 12, 24, 72 and 144 hpi were enzymatically digested and single cell suspensions were analyzed by flow cytometry for quantification of (**A**) alveolar macrophages (SiglecF$^+$ CD11c$^+$), (**B**) neutrophils (Ly-6G$^+$ CD11b$^+$) and (**C**) monocytes (Ly-6C$^+$ CD11b$^+$). All Results are shown as mean ± SEM (*n = 3*) and are representative of at least two independent experiments with similar results. Statistical significance was determined by one-way ANOVA with Bonferroni's test (ns = not significant, **p* < 0.05; ***p* < 0.01, ****p* < 0.001).

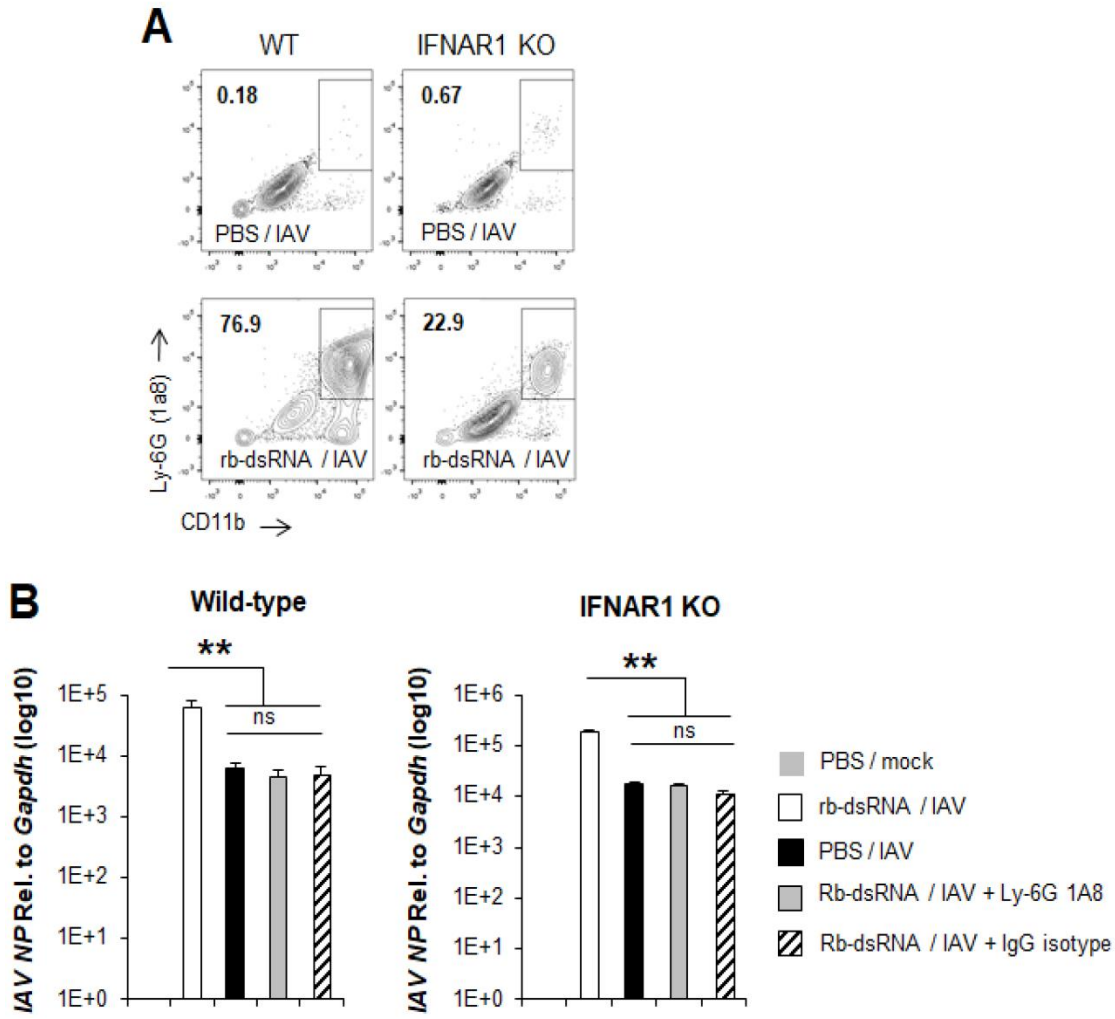

Figure 15. Residual antiviral activity in IFNAR1 deficient mice is independent of neutrophil

Wild-type B6 and IFNAR1 KO mice were treated with rb-dsRNA or not and infected with IAV. (**A**) Twenty-four hrs post-infection lungs were analyzed by flow cytometry for quantification of neutrophils in BAL fluid. (**B**) The respective mice were administered (i.n.) Ly-6G antibody (clone 1A8) 6 hrs after each dose of rb-dsRNA for the depletion of neutrophils. Lungs were harvested at 24 hpi and viral RNA quantified by qRT-PCR. All results are shown as mean ± SEM (*n* = *4*) and are representative of at least two independent experiments with similar results. Statistical significance was determined by one-way ANOVA with Bonferroni's test (ns = not significant, ** $p < 0.01$).

3.6. Rb-dsRNA induces a pyroptotic-like depletion of AMΦ via caspase-1 activation through TRIF

Besides induction of IFNs, recognition of viral RNA and analogues is associated with inflammatory signatures such as recruitment of inflammatory cells [12] and activation of the inflammasome[10, 19, 22] or alternative inflammatory and anticancer events[24, 55]. These responses have been shown to contribute to immunity. Considering that IFN-I only played a partial role in antiviral immune protection induced by rb-dsRNA and recruited neutrophils did not contribute the residual protection, we investigated the contribution of other dsRNA-induced events.

Because reduced AMΦ frequency after rb-dsRNA administration was observed, I sought to determine whether rb-dsRNA also induced cell death, particularly pyroptotic events *in vitro*. When mice were subjected to i.n. rb-dsRNA, macrophages in BAL exhibited cell death (Figure 16A). Similarly, stimulated bone-marrow derived (BM-MΦ) and AMΦ *in vitro* (Figure 16B, 16C, 16D) indicated that rb-dsRNA mediates spontaneous lactate dehydrogenase (LDH) release in the supernatant (Figure 16C and 16D), an event associated with pyroptosis. Unlike rb-dsRNA, poly I:C did not result in LDH release. In fact, in previous reports, *in vitro* LDH release induced by poly I:C on primary macrophages required the addition of ATP [22].

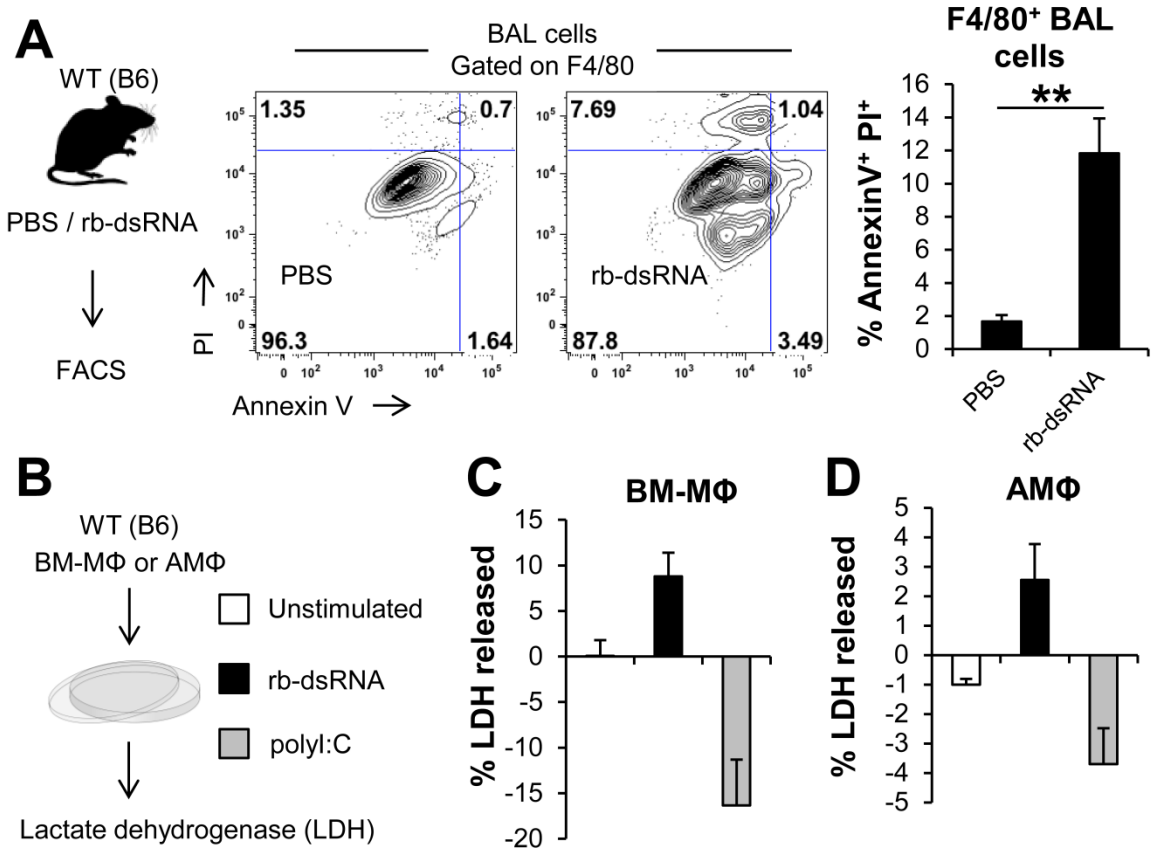

Figure 16. DsRNA induces macrophage death

(**A**) Wild-type B6 mice received PBS or rb-dsRNA as illustrated; 6hrs later BAL cells were analyzed by flow cytometry to quantify propiudium iodide^{+} (PI^{+}) and annexin V^{+} F4/80^{+} macrophages. (**B**) Bone-marrow derived (BM-MΦ) and alveolar macrophages (AMΦ) from B6 mice were stimulated or not with rb-dsRNA or poly I:C (10 µg/ml) as depicted. Percentage of LDH released from (**C**) BM-MΦ and (**D**) AMΦ was assessed 15 hrs later. Results are shown as mean ± SEM (*n = 4*) and are representative of at least two independent experiments with similar results. Statistical significance was determined by unpaired student *t-test* (ns = not significant, $^{**}p < 0.01$).

Next, using primary macrophages obtained from caspase-1-deficient mice, it was found that rb-dsRNA-induced LDH release is dependent on caspase-1 (Figure 17A). To further examine caspase-1 involvement, mice were treated with the caspase-1 inhibitor, Ac-YVAD-cmk, and stimulated with rb-dsRNA (Figure 17B).

Mice administered with rb-dsRNA showed an increased level of LDH in the BAL fluid, and this increase was abrogated by caspase-1 inhibition (Figure 17C). Likewise, cell death induced by rb-dsRNA was decreased by caspase-1 inhibition (Figure 17D). Immunoblot analysis of BAL cells confirmed caspase-1 activation (Figure 18A) and IL-1β release in the BAL fluid of rb-dsRNA-treated wild-type mice was confirmed by ELISA (Figure 18E). DsRNA have previously been shown to activate the inflammasome in macrophages subsequently resulting in caspase-1 activation[22]. To reveal the signaling cascade responsible for caspase-1 activation, different KO mice were treated with rb-dsRNA and the activation of caspase-1 was assessed. Rb-dsRNA-driven activation of caspase-1 was independent of the MDA5/IPS-1 axis (Figure 18B), but required TLR3/TRIF signaling (Figure 18C and 18D). MDA5 appeared to play a role, although not significantly, in IL-1β production, whereas TRIF-deficient mice completely lost the ability to produce detectable amounts of IL-1β in BAL fluid (Figure 18E). Considering that MDA5 did not contribute to caspase-1 activation, we speculated that its contribution to IL-1β production was at the mRNA level. Quantitative PCR revealed that although the TRIF signaling pathway was the dominant contributor to mRNA induction of IL-1β, MDA5 signaling also partially participated in transcriptional activation of IL-1β gene (Figure 18F).

These results suggest that in addition to IFN-I gene induction and production, rb-dsRNA triggers caspase-1 activation in AMΦ through TRIF signaling adaptor. This cascade of inflammatory events subsequently resulted in the release

of LDH and secretion of IL-1β, an event linked to pyroptosis. Release of LDH and IL-1β has been reported to depend on the cleavage of gasdermin D, the executioner of pyroptosis[56, 57, 58, 59]. To confirm whether or not gasdermin D cleavage is involved in the currently observations, this protein was investigated in BAL cells. Intranasal administration rb-dsRNA led to the cleavage of gasdermin D downstream of TRIF (Figure 18G), suggesting its involvement in dsRNA-induced pyroptosis.

Together, these results suggest that RNA-dependent activation of inflammatory caspases via TRIF controlled the cleavage of gasdermin D which subsequently facilitated the release of LDH and IL-1β as markers of a pyroptotic-like cell death.

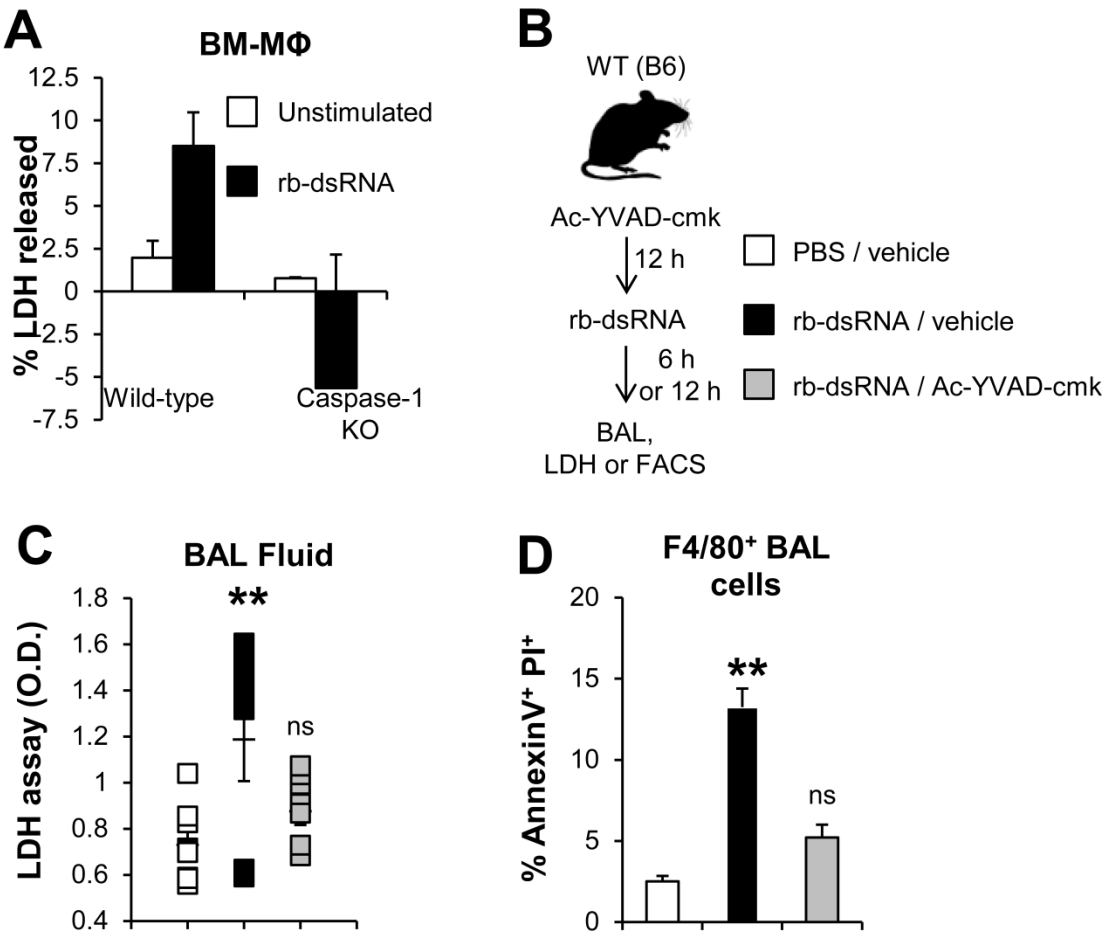

Figure 17. DsRNA-induced cell death is caspase-1-dependent

(**A**) Percentage LDH released from BM-MΦ from B6 and caspase-1 KO mice stimulated with rb-dsRNA (10 µg/ml) for 15 hrs. Results are shown as mean ± SEM (*n = 2*) and are representative of three independent experiments with comparable results. (**B**) B6 mice were treated with Ac-YVAD-cmk (10 mg/kg) or vehicle and inoculated with PBS or rb-dsRNA as illustrated. (**C**) LDH assay from BALF collected 12 hrs later was measured and shown as optical density (O.D.) (*n = 9*). (**D**) BAL cells were collected 6 hrs later for flow cytometry assesment of PI^+ and $AnnexinV^+$ cells. Results are representative of at least two independent experiments with comparable results. Statistical significance was determined by unpaired *t-test* and one-way ANOVA with Bonferroni's test (ns = not significant, $^{**}p < 0.01$)

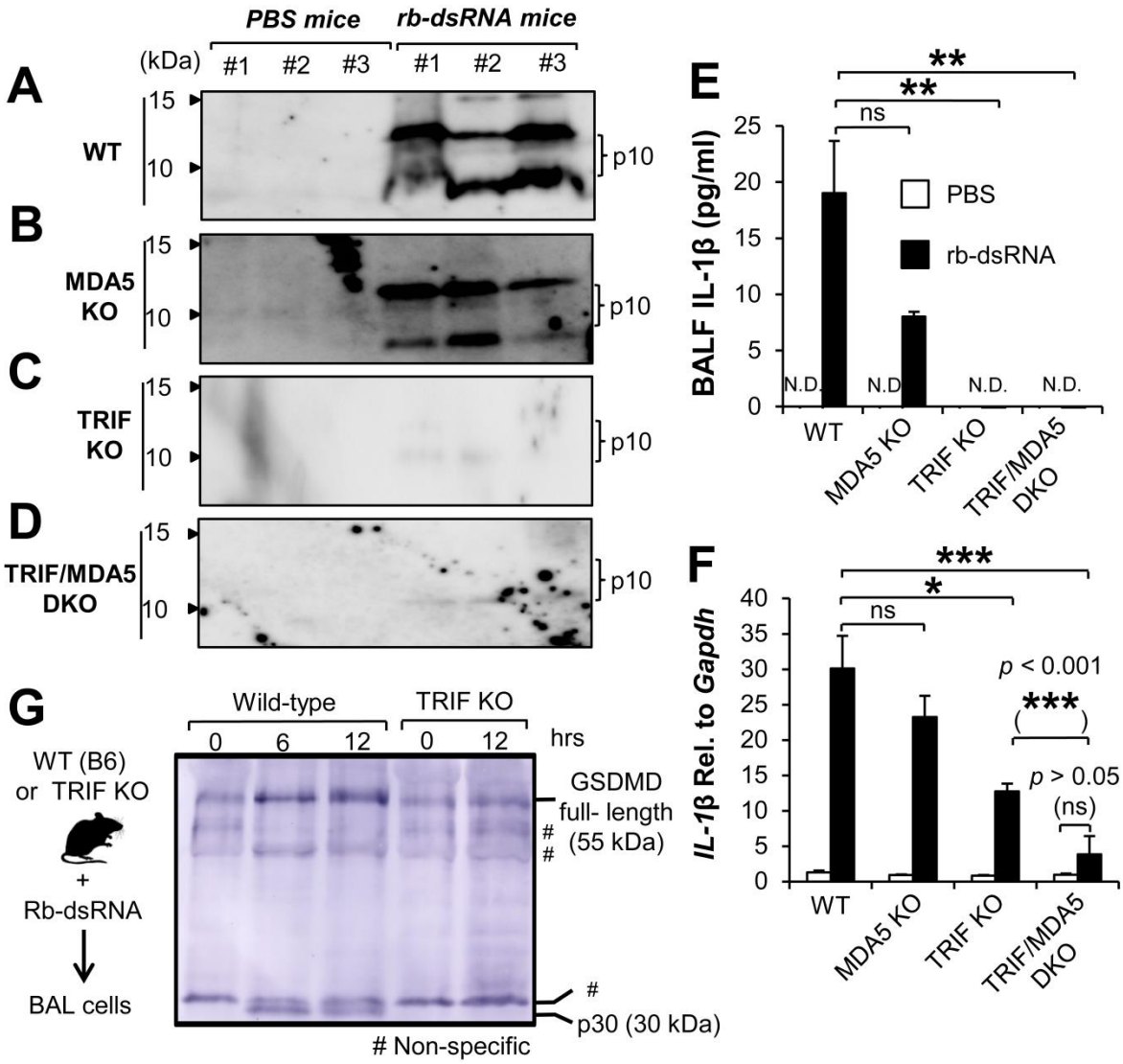

Figure 18. Rb-dsRNA activates caspase-1 in TRIF-dependent manner and drives a macrophage pyroptosis-like event

(**A-D**) Western blot of activated caspase-1 (p10) from lysate of BAL cells harvested 12 hrs post rb-dsRNA. (**E**) IL-1β ELISA of BAL fluids from (**A**), (**B**), (**C**), and (**D**). Results are shown as mean ± SEM (*n = 3*). (**F**) B6 and KO mice received rb-dsRNA and lungs were analyzed 4 hrs later. This time point corresponded to IL-1β mRNA peak. Results are shown as mean ± SEM (*n = 4 to 5*). (**G**) B6 mice received rb-dsRNA and BAL cells were collected 6 and 12 hours later. For TRIF KO mice only a single time point (12 hours) was taken. Western blot analysis of whole cell lysate from BAL cells was analyzed for gasdermin D cleavage. Results are representative of at least two independent experiments with comparable results. Statistical significance was determined by unpaired *t-test* and one-way ANOVA with Bonferroni's test (ns = not significant, **p* < 0.05; ***p* < 0.01, ****p* < 0.001).

3.7. Caspase-1 activation in alveolar macrophages contributes to rb-dsRNA-driven antiviral immunity

To further investigate whether rb-dsRNA-driven caspase-1 activation contributes to antiviral protection *in vivo*, mice were treated with the caspase-1 inhibitor and challenged with IAV. IAV replication was inhibited by rb-dsRNA treatment and inhibition of caspase-1 significantly reduced rb-dsRNA-driven antiviral activity (Figure 19A). Additionally, rb-dsRNA-induced antiviral activity was significantly reduced in caspase-1 KO mice (Figure 19B) without significantly affecting IFN-β induction (Figure 19C). These results suggest that caspase-1-dependent inflammatory response contributes to antiviral immune activity *in vivo* independently of IFN.

To reconcile IFN-I signaling and caspase-1 activation in rb-dsRNA-driven antiviral protection, IFNAR1 KO mice were administered the caspase-1 inhibitor. Partial protection by rb-dsRNA in IFNAR1 KO mice was abrogated by caspase-1 inhibition (Figure 19D), suggesting an IFN-independent, caspase-1-dependent role in antiviral protection. This observation prompted us to investigate the possible involvement of IL-1β. Inhibition of IL-1 signaling using the IL-1 receptor antagonist Anakinra proposed that the IFN-independent caspase-1-dependent residual antiviral protection in IFNAR1 KO mice was independent of IL-1 signaling (Figure 19E). Interestingly, IFNAR1 KO mice lost the ability to produce detectable amounts of IL-1β in BAL fluid (Figure 19F) and exhibited significantly lower induction of IL-1β mRNA (Figure 19G)[60]. This supported even more that IL-1β contribution to

antiviral protection in IFNAR1 KO was unlikely. Overall, the survival rate of IFNAR1 KO mice treated with rb-dsRNA was significantly lower in the presence of the caspase-1 inhibitor and comparable to TRIF/MDA5 DKO mice (Figure 20A).

All together these results suggest that in addition to IFN-I induction and signaling, rb-dsRNA activated caspase-1 which drives a pyroptotic-like cell depletion of AMΦ. Together these events were critical to mount a complete antiviral immune protection induced by rb-dsRNA against respiratory viruses.

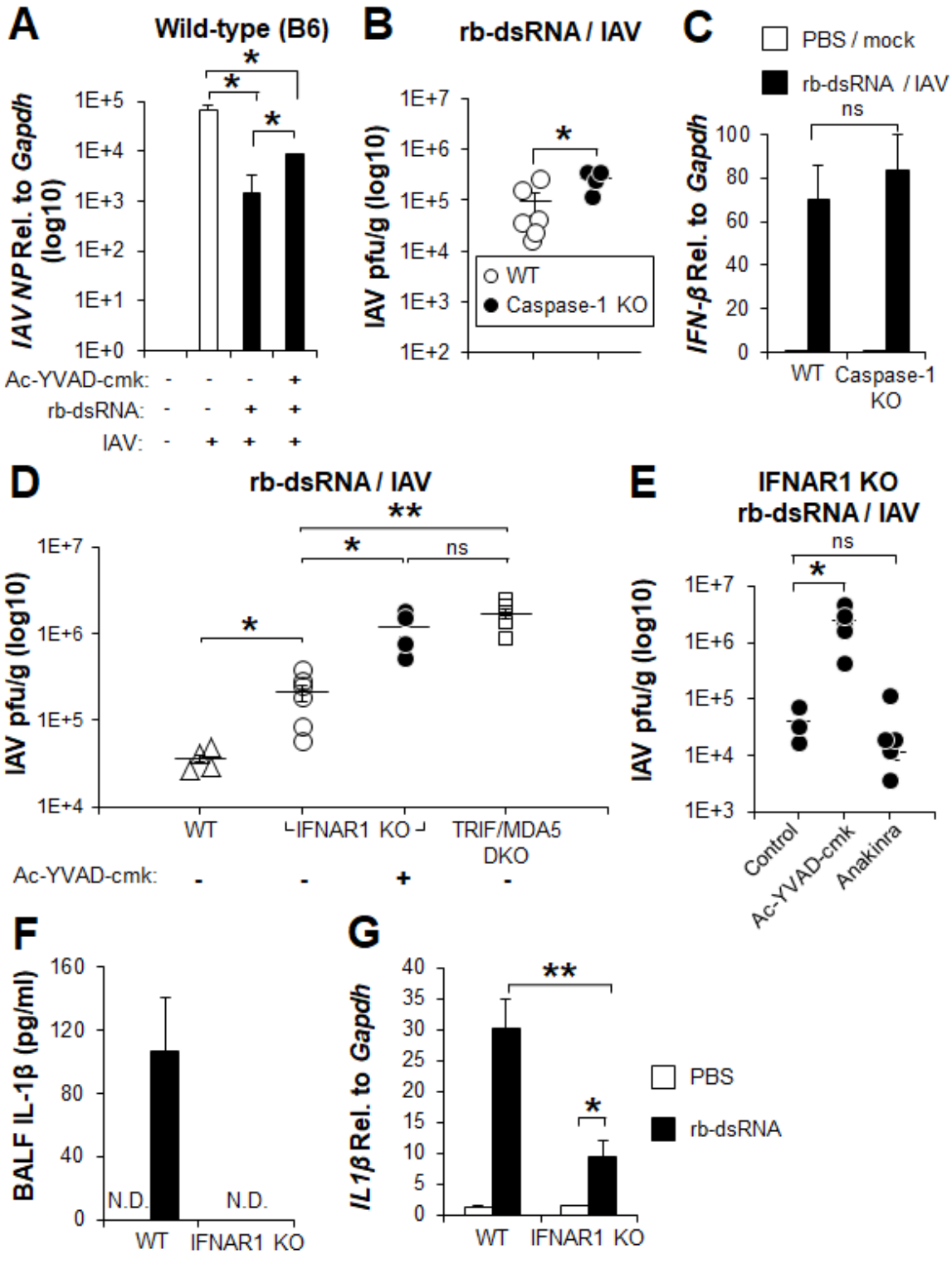

Legend on the next page

Figure 19. Rb-dsRNA-driven caspase1-activation contributes to antiviral activity

(**A**) Wild-type mice received Ac-YVAD-cmk before being treated or not with rb-dsRNA and infected with IAV. Lungs were harvested 24 hpi and analyzed by qRT-PCR. (**B**) Wild-type or caspase-1 KO mice were treated with rb-dsRNA and infected with IAV. Lungs were analyzed by plaque assay 24 hpi. (**C**) Lungs harvested from mice described in (**B**) were subjected to qRT-PCR for IFN-β mRNA. (**D**) IFNAR1 KO mice were treated with Ac-YVAD-cmk or DMSO before being treated with rb-dsRNA alongside with wild-type and TRIF/MDA5 DKO mice. Lungs were analyzed by plaque assay 24 hpi. (**E**) IFNAR1 KO mice were treated with Ac-YVAD-cmk or Anakinra (IL1RA), and treated with rb-dsRNA and infected with IAV. Lungs were analyzed by plaque assay 24 hpi. All results are shown as mean ± SEM (*n = 3 to 6*) and are representative of at least two independent experiments with similar results. Statistical significance was determined by unpaired student *t-test* and one-way ANOVA with Bonferroni's test (ns = not significant, **p* < 0.05; ***p* < 0.01).

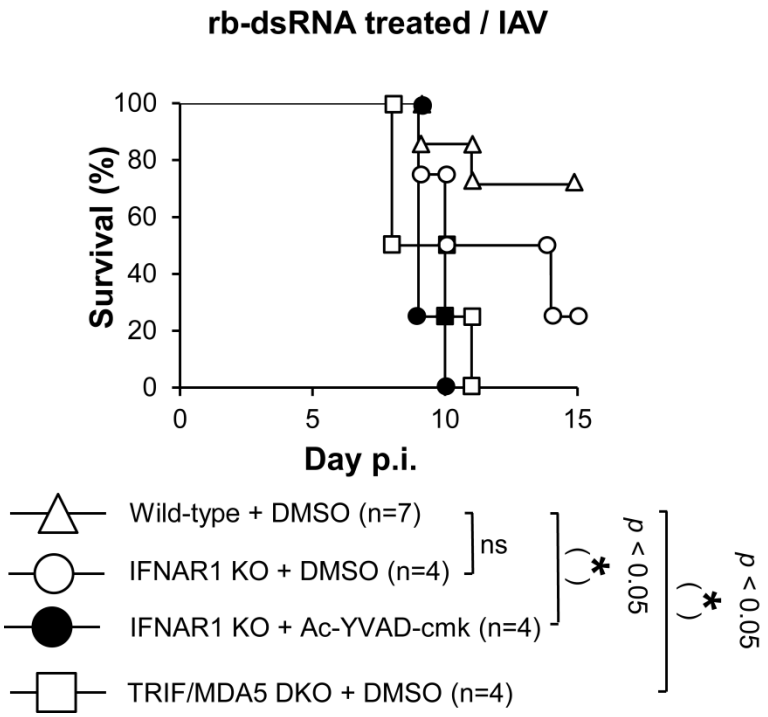

Figure 20. IFN-I signaling and caspase-1 together mount rb-dsRNA-driven immunity

Wild-type, IFNAR1 KO and TRIF/MDA5 DKO mice received Ac-YVAD-cmk or DMSO, were treated with rb-dsRNA and infected with IAV. Survival rate was monitored. All results are shown as mean ± SEM (*n = 3 to 6*) and are representative of at least two independent experiments with similar results. Statistical significance was determined by one-way ANOVA with Bonferroni's test (ns = not significant, **p* < 0.05).

Chapter 4

DISCUSSION

In this study, a novel immune stimulant capable of mounting a protection against lethal airway viral infection in mice is introduced. This ligand is of natural origin; therefore it might be a safer *in vivo* alternative to widely considered synthetic analogues. Since long dsRNA molecules generated during viral replication are often infectious and hard to obtain in large amount, the enzymatically-synthesized dsRNA, poly I:C, has been utilized for immunological investigation for many years. For this purpose, polynucleotide phosphorylase, an enzyme polymerizing NDP into polynucleotide in a template independent manner, was used. By annealing the resultant homopolymer, dsRNAs, such as poly A:U, poly C:G, and poly I:C, are obtained. Of these dsRNAs, poly I:C exhibited by far the strongest immune-stimulatory effect, indicating the importance of its unique nucleotide sequence; however, its mechanism is still unclear. It is suggested, therefore, that it may not mimic the precise biological activity of natural virus-derived dsRNA. Difficulty to synthesize high molecular weight RNA molecules has been a limitation for MDA5-related studies while RIG-I has been extensively studied and characterized. Although the reported natural dsRNA has been used in selected studies[61, 62] these investigations were limited to an *in vitro* assessment with no physiological relevance. Additionally, this study shows that the plant-derived long dsRNA activates MDA5 in addition to TLR3.

The current study revealed that rb-dsRNA exhibits a strong immune stimulating capacity in mice lungs. Although the nucleic acid stimulated immunity in other organs as well, this study focused solely on the respiratory tract. This is

because different organs exhibited diverse immune-stimulatory profiles probably due to the difference in resident immune cell populations. Additionally, intranasal administration provides a less invasive route of administration compared injections. In murine lungs, in addition to IFN-I, a panel of cytokines, chemokines, and antiviral proteins are induced by rb-dsRNA with respective kinetics and contribute to direct down-regulation of viral replication early after infection. MDA5- and TLR3-mediated signaling commonly regulates these genes. Rb-dsRNA treatment in mice suppressed subsequent IAV replication at an early time point. However, viral load was restored to indistinguishable difference levels at a later time. With the milder Sendai virus, suppression of viral replication was also reduced but persisted up to a later time of infection. It is of note that laboratory mice lack functional *mx1*, an IFN-inducible gene critical for resistance to IAV. Therefore, anti-IAV response mediated by IFN-I is genetically attenuated in laboratory mice. Nevertheless, the mice are capable of mounting protection against IAV by activating additional mechanisms.

Rb-dsRNA intranasal administration caused recruitment of neutrophils and monocytes in the lungs. This recruitment is partially dependent on IFN-I signaling probably through IFN-dependent induction of chemokines. In case of neutrophils, this accumulation was transient and no infiltrated neutrophils were evident after 3 days. In contrast to rb-dsRNA, replicating IAV may constantly provide ligands and cause inflammation resulting in prolonged infiltration of neutrophils throughout the course of infection. Although neutrophils have been shown to play a role in antiviral

innate immune responses[11, 53], antibody-mediated depletion of neutrophils immediately before and after rb-dsRNA i.n. administration did not affect antiviral protection in wild-type and IFNAR1 KO lungs (Figure 15). Similar to neutrophils, monocytes are transiently accumulated within 24 h of rb-dsRNA administration. In contrast, IAV infection gradually increased monocytes in the lungs. Rb-dsRNA-treated and IAV-infected mice exhibited biphasic accumulation of monocytes. However there is no evident correlation between accumulation of inflammatory monocytes and host survival. In contrast to infiltrated inflammatory cells, rb-dsRNA treatment transiently reduced AMΦ frequency; however it was completely recovered later. In contrast, lethal IAV infection depletes AMΦ population without full recovery. This depletion by IAV infection contributes to virus-induced morbidity and mortality[51, 52, 63]. Interestingly, rb-dsRNA treatment of IAV-infected mice allowed recovery of AMΦ depleted by IAV infection. Although not complete, this observation suggested that rb-dsRNA-driven re-population of AMΦ could contribute to host survival. It is possible that this phenomenon is directly linked to viral load during the early time of infection.

Further investigation of AMΦ depletion by rb-dsRNA demonstrated the critical involvement of caspase-1 in AMΦ and its role in the observed antiviral protection. This study suggests the importance of a caspase-1-mediated event in controlling RNA virus replications and host protection independently of both IFN-I and IFN-III (Figure 13D). Caspase-1 activation is specifically induced by TLR3 signaling through TRIF/RIPK/FADD and inflammasome activation[22], whereas the

MDA5-mediated signal does not activate inflammasome[10]. On the other hand, RIG-I, which is not stimulated by rb-dsRNA (Figure 3C) as demonstrated by MEF transfection experiment, has been reported to activate inflammasome[64]. The data from MEF transfection, in addition to the observation made using TRIF/MDA5 DKO, confirmed that rb-dsRNA is a ligand of MDA5 and TLR3 but not RIG-I. Since primary MEF do not express IL-1β, it was not possible to evaluate the production of IL-1β as a marker for inflammasome activation. However, since RIG-I-dependent inflammasome activation requires RIG-I activation by dsRNA recognition and no evidence of RIG-I activation (i.e. no IFN in DKO) was observed, it can be concluded that no subsequent activation of inflammasome by RIG-I was possible. Additionally, inflammasome-associated events in this study (i.e. caspase-1 activation, IL-1β production and gasdermin D cleavage) were exclusively TLR3/TRIF dependent (Figure 18). These results indicate that caspase-1 activation by rb-dsRNA through TLR3/TRIF spontaneously induces a pyroptosis-like cell death in macrophages, in contrast to poly I:C which requires addition of ATP[22]. Gasdermin D, which is the executor of pyroptosis, is also activated through TLR3/TRIF recognition and signaling (Figure 18).

Although the antiviral activity of pyroptosis has been proposed[65, 66], no definitive mechanism has been described so far. It is possible that cells, particularly macrophages, eliminate pathogens by dying after engulfment of pathogens. Another possibility is that pyroptotic cells release their cytoplasmic content, thereby enhancing inflammatory signals leading to recruitment of immune cells such as

neutrophils. Such mechanisms have been demonstrated in bacterial-induced pyroptosis[21, 23, 25, 67], while the observed antiviral mechanism of pyroptosis still needs to be clarified. These results also suggest that immune protection induced by rb-dsRNA was independent of IL-1β signaling since blockade of IL-1 receptor did not abolish the residual antiviral protection (Figure 19). Actually, absence of IFN-I signaling significantly reduces IL-1β mRNA induction in the lungs upon RNA stimulation (Figure 19) or RNA virus infection[60] thereby decreasing IL-1β impact. Caspase-1 activation, therefore, initiates an IL-1β-independent pyroptotic-like antiviral activity. Furthermore, this caspase-1-dependent antiviral activity was not related to IFN-I production since rb-dsRNA-driven induction of IFN-β was unchanged in mice deficient in caspase-1 compared to their wild-type counterparts (Figure 19B and 19C). Actually, caspase-1 has been shown to reduce IFN-I induction in response to DNA (and DNA viruses) by cleaving cGAS but not in response to RNA (and RNA viruses)[68].

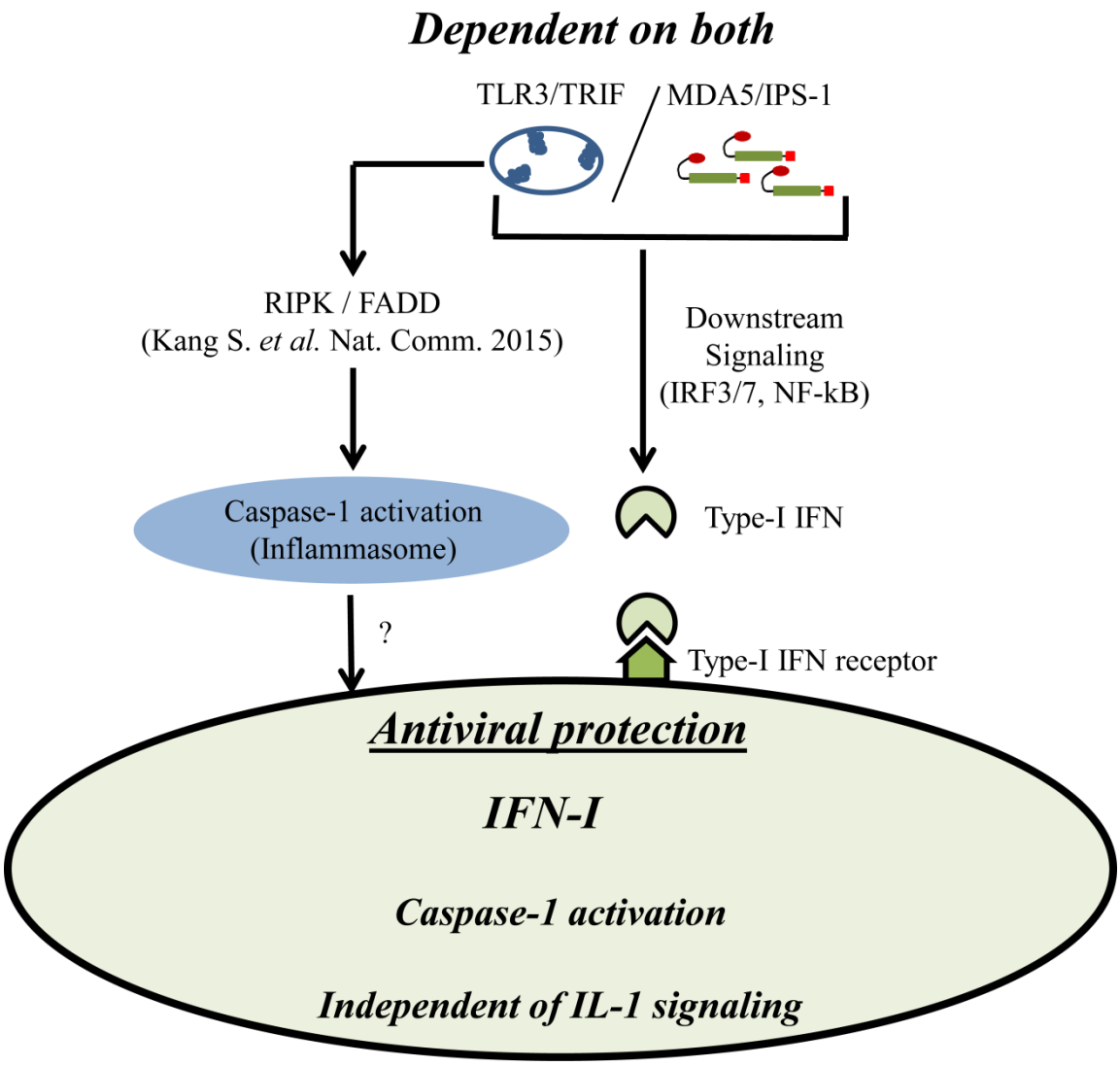

Figure 21. Summary of rb-dsRNA-induced antiviral activity

Rb-dsRNA recognition by TLR3 and MDA5 in alveolar macrophages activates type-I IFN induction. Binding of type-I IFN to its receptor in a paracrine and autocrine manner activates the antiviral state induced by rb-dsRNA. In parallel, activation of TLR3/TRIF by rb-dsRNA also spontaneously activates caspase-1 (inflammasome) and pyroptosis of alveolar macrophages. As a result, activation of caspase-1 resulted in the release of IL-1β and LDH to the extracellular space. Caspase-1 activation by rb-dsRNA contributed to the observed antiviral protection while IL-1 signaling did not seem to be involved.

In summary, this study proposes a new TLR3 and MDA5 ligand for both *in vitro* and *in vivo* studies of the immune system. It is able to activate antiviral immunity against respiratory viruses by reconciling IFN-I with direct antiviral activity and an inflammatory event, which may facilitate recovery as well as immobilization of acquired immune responses. This study also highlights the important role of both anti- and pro-inflammatory cascades in mounting an efficient immune response as two sides of the same coin; with the balance between the two being of paramount importance.

In the farming industry and in clinical settings, rb-dsRNA could provide a degree of protection to unvaccinated hosts in the center of a respiratory virus outbreak. This study opens doors to several nucleic acid-based therapeutic studies including anticancer and treatment of inflammatory diseases such as multiple sclerosis. Further studies will clarify the immune-modulating capacity of this dsRNA in other body tissues in addition to the lungs. This dsRNA also offers a much needed study material for biochemical investigations of MDA5 and its RNA recognition and signaling properties.

REFERENCES

1. Weber F, Wagner V, Rasmussen SB, Hartmann R, Paludan SR. Double-stranded RNA is produced by positive-strand RNA viruses and DNA viruses but not in detectable amounts by negative-strand RNA viruses. *Journal of virology* 2006, **80**(10)**:** 5059-5064.

2. Alexopoulou L, Holt AC, Medzhitov R, Flavell RA. Recognition of double-stranded RNA and activation of NF-kappaB by Toll-like receptor 3. *Nature* 2001, **413**(6857)**:** 732-738.

3. Yoneyama M, Kikuchi M, Natsukawa T, Shinobu N, Imaizumi T, Miyagishi M*, et al.* The RNA helicase RIG-I has an essential function in double-stranded RNA-induced innate antiviral responses. *Nature immunology* 2004, **5**(7)**:** 730-737.

4. Ranjan P, Bowzard JB, Schwerzmann JW, Jeisy-Scott V, Fujita T, Sambhara S. Cytoplasmic nucleic acid sensors in antiviral immunity. *Trends in molecular medicine* 2009, **15**(8)**:** 359-368.

5. Yoneyama M, Fujita T. Recognition of viral nucleic acids in innate immunity. *Reviews in medical virology* 2010, **20**(1)**:** 4-22.

6. Isaacs A. Antiviral Action of Interferon. *British medical journal* 1962, **2**(5301)**:** 353-355.

7. Merigan TC, Finkelstein MS. Interferon-stimulating and in vivo antiviral effects of various synthetic anionic polymers. *Virology* 1968, **35**(3)**:** 363-374.

8. Kern ER, Glasgow LA. Evaluation of interferon and interferon inducers as antiviral agents: animal studies. *Pharmacology & therapeutics* 1981, **13**(1)**:** 1-38.

9. Goritzka M, Makris S, Kausar F, Durant LR, Pereira C, Kumagai Y*, et al.* Alveolar macrophage-derived type I interferons orchestrate innate immunity to RSV through recruitment of antiviral monocytes. *The Journal of experimental medicine* 2015, **212**(5)**:** 699-714.

10. Rajan JV, Warren SE, Miao EA, Aderem A. Activation of the NLRP3 inflammasome by intracellular poly I:C. *FEBS letters* 2010, **584**(22)**:** 4627-4632.

11. Tate MD, Deng YM, Jones JE, Anderson GP, Brooks AG, Reading PC. Neutrophils ameliorate lung injury and the development of severe disease during influenza infection. *Journal of immunology* 2009, **183**(11)**:** 7441-7450.

12. Harris P, Sridhar S, Peng R, Phillips JE, Cohn RG, Burns L*, et al.* Double-stranded RNA induces molecular and inflammatory signatures that are directly relevant to COPD. *Mucosal immunology* 2013, **6**(3)**:** 474-484.

13. Field AK, Young CW, Krakoff IH, Tytell AA, Lampson GP, Nemes MM*, et al.* Induction of interferon in human subjects by poly I:C. *Proceedings of the Society for Experimental Biology and Medicine Society for Experimental Biology and Medicine* 1971, **136**(4)**:** 1180-1186.

14. Nemes MM, Tytell AA, Lampson GP, Field AK, Hilleman MR. Inducers of interferon and host resistance. VI. Antiviral efficacy of poly I:C in animal models. *Proceedings of the Society for Experimental Biology and Medicine Society for Experimental Biology and Medicine* 1969, **132**(2)**:** 776-783.

15. Caskey M, Lefebvre F, Filali-Mouhim A, Cameron MJ, Goulet JP, Haddad EK*, et al.* Synthetic double-stranded RNA induces innate immune responses similar to a live viral vaccine in humans. *The Journal of experimental medicine* 2011, **208**(12)**:** 2357-2366.

16. Matsukura S, Kokubu F, Kurokawa M, Kawaguchi M, Ieki K, Kuga H*, et al.* Synthetic double-stranded RNA induces multiple genes related to inflammation through Toll-like receptor 3 depending on NF-kappaB and/or IRF-3 in airway epithelial cells. *Clinical and experimental allergy : journal of the British Society for Allergy and Clinical Immunology* 2006, **36**(8)**:** 1049-1062.

17. Ota K, Kawaguchi M, Fujita J, Kokubu F, Huang SK, Morishima Y*, et al.* Synthetic double-stranded RNA induces interleukin-32 in bronchial epithelial cells. *Experimental lung research* 2015, **41**(6)**:** 335-343.

18. Ruane D, Brane L, Reis BS, Cheong C, Poles J, Do Y*, et al.* Lung dendritic cells induce migration of protective T cells to the gastrointestinal tract. *The Journal of experimental medicine* 2013, **210**(9)**:** 1871-1888.

19. Allen IC, Scull MA, Moore CB, Holl EK, McElvania-TeKippe E, Taxman DJ*, et al.* The NLRP3 inflammasome mediates in vivo innate immunity to influenza A virus through recognition of viral RNA. *Immunity* 2009, **30**(4)**:** 556-565.

20. Chakrabarti A, Banerjee S, Franchi L, Loo YM, Gale M, Jr., Nunez G*, et al.* RNase L activates the NLRP3 inflammasome during viral infections. *Cell host & microbe* 2015, **17**(4)**:** 466-477.

21. Jorgensen I, Zhang Y, Krantz BA, Miao EA. Pyroptosis triggers pore-induced intracellular traps (PITs) that capture bacteria and lead to their clearance by efferocytosis. *The Journal of experimental medicine* 2016, **213**(10)**:** 2113-2128.

22. Kang S, Fernandes-Alnemri T, Rogers C, Mayes L, Wang Y, Dillon C*, et al.* Caspase-8 scaffolding function and MLKL regulate NLRP3 inflammasome activation downstream of TLR3. *Nature communications* 2015, **6:** 7515.

23. Miao EA, Leaf IA, Treuting PM, Mao DP, Dors M, Sarkar A*, et al.* Caspase-1-induced pyroptosis is an innate immune effector mechanism against intracellular bacteria. *Nature immunology* 2010, **11**(12)**:** 1136-1142.

24. Nogusa S, Thapa RJ, Dillon CP, Liedmann S, Oguin TH, 3rd, Ingram JP*, et al.* RIPK3 Activates Parallel Pathways of MLKL-Driven Necroptosis and FADD-Mediated Apoptosis to Protect against Influenza A Virus. *Cell host & microbe* 2016, **20**(1)**:** 13-24.

25. Qu Y, Misaghi S, Newton K, Maltzman A, Izrael-Tomasevic A, Arnott D*, et al.* NLRP3 recruitment by NLRC4 during Salmonella infection. *The Journal of experimental medicine* 2016, **213**(6)**:** 877-885.

26. Roberson EC, Tully JE, Guala AS, Reiss JN, Godburn KE, Pociask DA*, et al.* Influenza induces endoplasmic reticulum stress, caspase-12-dependent

apoptosis, and c-Jun N-terminal kinase-mediated transforming growth factor-beta release in lung epithelial cells. *American journal of respiratory cell and molecular biology* 2012, **46**(5)**:** 573-581.

27. Coutts RH. First report of an endornavirus in the Cucurbitaceae. *Virus genes* 2005, **31**(3)**:** 361-362.

28. Horiuchi H, Moriyama H, Fukuhara T. Inheritance of Oryza sativa endornavirus in F1 and F2 hybrids between japonica and indica rice. *Genes & genetic systems* 2003, **78**(3)**:** 229-234.

29. Lim S, Kim KH, Zhao F, Yoo RH, Igori D, Lee SH*, et al.* Complete genome sequence of a novel endornavirus isolated from hot pepper. *Archives of virology* 2015, **160**(12)**:** 3153-3156.

30. Okada R, Kiyota E, Moriyama H, Fukuhara T, Valverde RA. Molecular and biological properties of an endornavirus infecting winged bean (Psophocarpus tetragonolobus). *Virus genes* 2016.

31. Okada R, Kiyota E, Sabanadzovic S, Moriyama H, Fukuhara T, Saha P*, et al.* Bell pepper endornavirus: molecular and biological properties, and occurrence in the genus Capsicum. *The Journal of general virology* 2011, **92**(Pt 11)**:** 2664-2673.

32. Fukuhara T, Koga R, Aoki N, Yuki C, Yamamoto N, Oyama N*, et al.* The wide distribution of endornaviruses, large double-stranded RNA replicons with plasmid-like properties. *Archives of virology* 2006, **151**(5)**:** 995-1002.

33. Osaki H, Nakamura H, Sasaki A, Matsumoto N, Yoshida K. An endornavirus from a hypovirulent strain of the violet root rot fungus, Helicobasidium mompa. *Virus research* 2006, **118**(1-2)**:** 143-149.

34. Moriyama H, Nitta T, Fukuhara T. Double-stranded RNA in rice: a novel RNA replicon in plants. *Molecular & general genetics : MGG* 1995, **248**(3)**:** 364-369.

35. Iannitti RG, Napolioni V, Oikonomou V, De Luca A, Galosi C, Pariano M*, et al.* IL-1 receptor antagonist ameliorates inflammasome-dependent inflammation in murine and human cystic fibrosis. *Nature communications* 2016, **7:** 10791.

36. Liu X, Zhang Z, Ruan J, Pan Y, Magupalli VG, Wu H*, et al.* Inflammasome-activated gasdermin D causes pyroptosis by forming membrane pores. *Nature* 2016, **535**(7610)**:** 153-158.

37. Petrasek J, Bala S, Csak T, Lippai D, Kodys K, Menashy V*, et al.* IL-1 receptor antagonist ameliorates inflammasome-dependent alcoholic steatohepatitis in mice. *The Journal of clinical investigation* 2012, **122**(10)**:** 3476-3489.

38. Kato H, Takeuchi O, Sato S, Yoneyama M, Yamamoto M, Matsui K*, et al.* Differential roles of MDA5 and RIG-I helicases in the recognition of RNA viruses. *Nature* 2006, **441**(7089)**:** 101-105.

39. Kato H, Takeuchi O, Mikamo-Satoh E, Hirai R, Kawai T, Matsushita K*, et al.* Length-dependent recognition of double-stranded ribonucleic acids by retinoic acid-inducible gene-I and melanoma differentiation-associated gene 5. *The Journal of experimental medicine* 2008, **205**(7)**:** 1601-1610.

40. Van Damme N, Goff D, Katsura C, Jorgenson RL, Mitchell R, Johnson MC*, et al.* The interferon-induced protein BST-2 restricts HIV-1 release and is downregulated from the cell surface by the viral Vpu protein. *Cell host & microbe* 2008, **3**(4)**:** 245-252.

41. Desai TM, Marin M, Chin CR, Savidis G, Brass AL, Melikyan GB. IFITM3 restricts influenza A virus entry by blocking the formation of fusion pores following virus-endosome hemifusion. *PLoS pathogens* 2014, **10**(4)**:** e1004048.

42. Brass AL, Huang IC, Benita Y, John SP, Krishnan MN, Feeley EM*, et al.* The IFITM proteins mediate cellular resistance to influenza A H1N1 virus, West Nile virus, and dengue virus. *Cell* 2009, **139**(7)**:** 1243-1254.

43. Kumar P, Sweeney TR, Skabkin MA, Skabkina OV, Hellen CU, Pestova TV. Inhibition of translation by IFIT family members is determined by their ability to interact selectively with the 5'-terminal regions of cap0-, cap1- and 5'ppp-mRNAs. *Nucleic acids research* 2014, **42**(5)**:** 3228-3245.

44. Daffis S, Szretter KJ, Schriewer J, Li J, Youn S, Errett J*, et al.* 2'-O methylation of the viral mRNA cap evades host restriction by IFIT family members. *Nature* 2010, **468**(7322)**:** 452-456.

45. Dittmann M, Hoffmann HH, Scull MA, Gilmore RH, Bell KL, Ciancanelli M*, et al.* A serpin shapes the extracellular environment to prevent influenza A virus maturation. *Cell* 2015, **160**(4)**:** 631-643.

46. Kumagai Y, Takeuchi O, Kato H, Kumar H, Matsui K, Morii E*, et al.* Alveolar macrophages are the primary interferon-alpha producer in pulmonary infection with RNA viruses. *Immunity* 2007, **27**(2)**:** 240-252.

47. Byrne AJ, Mathie SA, Gregory LG, Lloyd CM. Pulmonary macrophages: key players in the innate defence of the airways. *Thorax* 2015, **70**(12)**:** 1189-1196.

48. Byrne AJ, Maher TM, Lloyd CM. Pulmonary Macrophages: A New Therapeutic Pathway in Fibrosing Lung Disease? *Trends in molecular medicine* 2016, **22**(4)**:** 303-316.

49. Short KR, Kroeze EJ, Fouchier RA, Kuiken T. Pathogenesis of influenza-induced acute respiratory distress syndrome. *The Lancet Infectious diseases* 2014, **14**(1)**:** 57-69.

50. Le Goffic R, Balloy V, Lagranderie M, Alexopoulou L, Escriou N, Flavell R*, et al.* Detrimental contribution of the Toll-like receptor (TLR)3 to influenza A virus-induced acute pneumonia. *PLoS pathogens* 2006, **2**(6)**:** e53.

51. Schneider C, Nobs SP, Heer AK, Kurrer M, Klinke G, van Rooijen N*, et al.* Alveolar macrophages are essential for protection from respiratory failure and associated morbidity following influenza virus infection. *PLoS pathogens* 2014, **10**(4)**:** e1004053.

52. Tate MD, Pickett DL, van Rooijen N, Brooks AG, Reading PC. Critical role of airway macrophages in modulating disease severity during influenza virus infection of mice. *Journal of virology* 2010, **84**(15)**:** 7569-7580.

53. Tumpey TM, Garcia-Sastre A, Taubenberger JK, Palese P, Swayne DE, Pantin-Jackwood MJ*, et al.* Pathogenicity of influenza viruses with genes from the 1918 pandemic virus: functional roles of alveolar macrophages and neutrophils in limiting virus replication and mortality in mice. *Journal of virology* 2005, **79**(23)**:** 14933-14944.

54. Daley JM, Thomay AA, Connolly MD, Reichner JS, Albina JE. Use of Ly6G-specific monoclonal antibody to deplete neutrophils in mice. *Journal of leukocyte biology* 2008, **83**(1)**:** 64-70.

55. Kumar S, Ingle H, Mishra S, Mahla RS, Kumar A, Kawai T*, et al.* IPS-1 differentially induces TRAIL, BCL2, BIRC3 and PRKCE in type I interferons-dependent and -independent anticancer activity. *Cell death & disease* 2015, **6:** e1758.

56. Ding J, Wang K, Liu W, She Y, Sun Q, Shi J*, et al.* Pore-forming activity and structural autoinhibition of the gasdermin family. *Nature* 2016, **535**(7610)**:** 111-116.

57. He WT, Wan H, Hu L, Chen P, Wang X, Huang Z*, et al.* Gasdermin D is an executor of pyroptosis and required for interleukin-1beta secretion. *Cell research* 2015, **25**(12)**:** 1285-1298.

58. Kayagaki N, Stowe IB, Lee BL, O'Rourke K, Anderson K, Warming S*, et al.* Caspase-11 cleaves gasdermin D for non-canonical inflammasome signalling. *Nature* 2015, **526**(7575)**:** 666-671.

59. Sborgi L, Ruhl S, Mulvihill E, Pipercevic J, Heilig R, Stahlberg H*, et al.* GSDMD membrane pore formation constitutes the mechanism of pyroptotic cell death. *The EMBO journal* 2016, **35**(16)**:** 1766-1778.

60. Goritzka M, Durant LR, Pereira C, Salek-Ardakani S, Openshaw PJ, Johansson C. Alpha/beta interferon receptor signaling amplifies early

proinflammatory cytokine production in the lung during respiratory syncytial virus infection. *Journal of virology* 2014, **88**(11)**:** 6128-6136.

61. Lai Y, Adhikarakunnathu S, Bhardwaj K, Ranjith-Kumar CT, Wen Y, Jordan JL*, et al.* LL37 and cationic peptides enhance TLR3 signaling by viral double-stranded RNAs. *PloS one* 2011, **6**(10)**:** e26632.

62. Lai Y, Yi G, Chen A, Bhardwaj K, Tragesser BJ, Rodrigo AV*, et al.* Viral double-strand RNA-binding proteins can enhance innate immune signaling by toll-like Receptor 3. *PloS one* 2011, **6**(10)**:** e25837.

63. Coulombe F, Jaworska J, Verway M, Tzelepis F, Massoud A, Gillard J*, et al.* Targeted prostaglandin E2 inhibition enhances antiviral immunity through induction of type I interferon and apoptosis in macrophages. *Immunity* 2014, **40**(4)**:** 554-568.

64. Poeck H, Bscheider M, Gross O, Finger K, Roth S, Rebsamen M*, et al.* Recognition of RNA virus by RIG-I results in activation of CARD9 and inflammasome signaling for interleukin 1 beta production. *Nature immunology* 2010, **11**(1)**:** 63-69.

65. Doitsh G, Galloway NL, Geng X, Yang Z, Monroe KM, Zepeda O*, et al.* Cell death by pyroptosis drives CD4 T-cell depletion in HIV-1 infection. *Nature* 2014, **505**(7484)**:** 509-514.

66. Galloway NL, Doitsh G, Monroe KM, Yang Z, Munoz-Arias I, Levy DN*, et al.* Cell-to-Cell Transmission of HIV-1 Is Required to Trigger Pyroptotic Death of Lymphoid-Tissue-Derived CD4 T Cells. *Cell reports* 2015, **12**(10)**:** 1555-1563.

67. Miao EA, Alpuche-Aranda CM, Dors M, Clark AE, Bader MW, Miller SI*, et al.* Cytoplasmic flagellin activates caspase-1 and secretion of interleukin 1beta via Ipaf. *Nature immunology* 2006, **7**(6)**:** 569-575.

68. Wang Y, Ning X, Gao P, Wu S, Sha M, Lv M*, et al.* Inflammasome Activation Triggers Caspase-1-Mediated Cleavage of cGAS to Regulate Responses to DNA Virus Infection. *Immunity* 2017, **46**(3)**:** 393-404.

ACKNOWLEDGEMENTS

First and foremost I would like to thank the Almighty God for the strength and blessings renewed daily. Secondly, I express my sincere gratitude to my wife without whom this achievement would not have been possible. Her strength, support and patience drove me every day.

I would like to extend my sincere gratitude to Dr. Takashi Fujita who, so kindly, mentored and supported me through my PhD studies. I also thank him for recruiting me under his mentorship; it has been an honor for me. My gratitude also goes to Dr. Hiroki Kato for his mentoring in and outside the laboratory. Furthermore, I would like to thank Mr. Fumitaka Miyoshi for his help establishing the rb-dsRNA extraction protocol, Dr. Michaela Weber for her advice and support during a time of uncertainty in my PhD studies. My deepest gratitude also goes to Dr. James Hejna for his training in scientific writing and communication, and Dr. Sergei V. Kotenko for providing the IL-28αR$^{-/-}$ for this study.

This study was supported by research grants from the Ministry of Education, Culture, Sports, Science, and Technology of Japan: Innovative Areas “Infection Competency”#24115004 (T.F.).

This thesis is based on material contained in the following scholarly paper:

Dacquin M. Kasumba; Takara Hajake; Seong-Wook Oh; Sergei V. Kotenko; Hiroki Kato; Takashi Fujita

A plant-derived nucleic acid reconciles type-I IFN and a pyroptotic-like event in immunity against respiratory viruses

Journal of Immunology. 2017, 199 (7) 2460-2474